2017

# Feasibility & Discovery using FOX System to Generate Gain-of-Function Mutations with Hybrid Poplars

James Rauschendorfer
*Michigan Technological University*, jkrausch@mtu.edu

# FEASIBILITY & DISCOVERY USING FOX SYSTEM TO GENERATE GAIN-OF-FUNCTION MUTATIONS WITH HYBRID POPLARS

By

James Karl Rauschendorfer

A THESIS

Submitted in partial fulfillment of the requirements for the degree of

MASTER OF SCIENCE

In Forest Molecular Genetics & Biotechnology

MICHIGAN TECHNOLOGICAL UNIVERSITY

2017

This thesis has been approved in partial fulfillment of the requirements for the Degree of MASTER OF SCIENCE in Forest Molecular Genetics and Biotechnology.

School of Forest Resources and Environmental Science

| | |
|---|---|
| Thesis Advisor: | *Dr. Victor Busov* |
| Committee Member: | *Dr. Molly Cavaleri* |
| Committee Member: | *Dr. Hairong Wei* |
| School Dean: | *Dr. Terry Sharik* |

# Table of Contents

# Acknowledgements

**To my parents, sister and brother:**

Thank you for your continued support through everything. I love you all.

**To the faculty, staff and students of MTU's SFRES:**

Thank you for taking me into your community.

**To Galina Agapova and Professor Tanya Georgiana:**

I cannot thank both of you enough for your support in my experiments.

**To Professor Victor Busov:**

Thank you for all the direction, advice and inspiration in the past years. You're a brilliant scientist. Your guidance made this all possible.

# List of Abbreviations

β-ME – β-Mercaptoethanol
$\Delta\Delta C_t$ – Comparative $C_t$ Method
20th – 20 Internode
AGI – *Arabidopsis* Gene ID
AMP – Adenosie Monophosphate
AT – Activation Tagging
*At – Arabidopsis Thaliana*
ATV – Activation Tagging Vector
bHLH – Basic Helix Loop Helix
BLAST – Basic Local Alignment Sequencing Tool
BSR1 – Broad Spectrum Resistance 1
C5 – Cellulose
C6 – Hemicellulose
CaMV – Cauliflower Mosaic Virus
cDNA – Complementary DNA
CKX – CYTOKININ OXIDASE
CZ – Cambial Zone
DMAPP – dimethylallyl diphosphate
dNTP – deoxynucleotide triphosphates
Den-g – Density Green Stem
Den-d – Density Dry Stem
DNA – Deoxyribonucleic Acid
DW – Dry Weight
DUF – Domain of Unknown Function
EB1 – Elution Buffer 1
EB2 – Elution Buffer 2
EDTA – Ethylenediamine tetraacetic acid
EtOH – Ethanol
*F* – Mutant FOX
*F* – Non-Phenotypic FOX
FOX – Full-Length cDNA Overexpression
FLA – FASCICLIN-LIKE ARABINOGLACTAN PROTEIN
fl-cDNA – Full-Length cDNA
gDNA – Genomic DNA
GA2ox – GIBERRELLIN 2-OXIDASE
GF – Gain-of-Function
GO – Gene Ontology
iP – Isopentenyl Adenine
iPR – iP Riboside
iPRMP – Isopentenyl Adenosine Monophosphate
IPT – ISOPENTYL TRANSFERASE
IRX – IRREGULAR XYLEM

LF – Loss-of-Function
LHW – LONESOME HIGHWAY
LOG – LONGLY GUY
MAP – MICROTUBULE ASSOCIATED PROTEIN
MC% – Moisture Content Percentage
MCS – Multiple Cloning Site
$MgSO_4$ – Magnesium Sulfate
MM – Master Mix
mRNA – Messenger RNA
MYB – MYB DOMAIN PROTEIN 103
m/z – Mass to Charge Ratio
NaCl – Sodium Chloride
OE – Overexpression
OCS – Octopine Synthase
P – Pith
PCD – Programmed cell death
PCR – Polymerase Chain Reaction
Ph – Phloem
*Pt – Populus Trichocarpa*
*Pta – Populus tremula X alba*
PVP – Polyvinylpyrrolidone
PyMBMS – Pyrolysis Molecular-Beam Mass Spectrometry
qRT-PCR – Quantitative Real Time PCR
RNA – Ribonucleic Acid
RNA-seq – RNA Sequencing
rpm – Revolutions per Minute
RT – Reverse Transcriptase
RXN – Reaction
SCW – Secondary Cell Wall
SDS – Sodium Dodecyl Sulfate
SOC – Super Optimal Broth with Catabolite Repression
$T_0$ – Primary Transformant
T5L1 – TMO5-LIKE 1
TAE – Tris Base, Acetic Acid and EDTA Buffer
T-DNA – Transfer DNA
TMO5 – TARGET OF MONOPTEROS 5
TRIS HCl – Tris Hydrochloride
UPGMA – Unweighted Pair Group Method with Arithmetic Mean
wt 717 – Wild Type 717
X – Xylem

## Abstract

The Full-length complementary DNA OvereXpression (FOX) system is an approach to generating gain-of-function (GF) plants predominantly used for studying *Arabidopsis*. This approach inserts T-DNAs containing random full-length complementary DNA (fl-cDNA) with upstream promoter and downstream terminator into the host plant genome. Studies using this method report the success generating overexpression populations with high mutation rates. We choose to investigate the feasibility and effectiveness of this method using poplars. We suspected using a succulent xylem specific fl-cDNAs library would enrich the transformant poplars with mutants affected in traits specific to woody tissue development. We observed a characteristically high mutation rate (17.7%) significantly enriched for mutants with altered cell wall composition. We determined selection of tissues for RNA sampling greatly influence types of genes inserted and phenotypes observed, as seen by the enrichment for FOX mutants affected in traits liked to developing xylem. Furthermore, using the FOX system we discovered overexpression of a fl-cDNA homologous for poplar specific LONELY GUY 1 (LOG1) resulted in a near doubling of stem xylem width. LOG1 belongs to a gene family encoding enzymes that directly convert inactive cytokinins to their active conformations. Examining stem sections, we determined LOG1 overexpression greatly increased active cytokinin concentration causing xylem proliferation. Complete phenotype recapitulation for LOG1 FOX line using Gateway OE method validated the feasibility of the FOX system for studying poplars.

# 1 Introduction

## 1.1 Economic & Environmental Value of Poplars

The *Populus* genus comprises over 30 species, spans a majority of the temperate regions of the US and is of great environmental importance (Dickmann 2001, Brunner, Busov, and Strauss 2004). Poplars have also become model organisms for understanding tree biology due to available resources and specific biological features: these include facile clonal propagation, fast growth, and transformability (Busov et al. 2005, Brunner, Busov, and Strauss 2004). In addition, poplar has a high quality whole genome sequence and annotation (Tuskan et al. 2006) that facilitates both functional and comparative genomic analysis of traits. Using both genomic studies and hybridized species, the *Populus* genus provides a toolset for understanding complex traits specific to trees of economic and environmental importance (Tuskan et al. 2006).

## 1.2 Mutagenesis Approaches for Functional Gene Discovery

One feature making the poplar unique among other tree taxa is its amenability to mutagenesis by *Agrobacterium* transformation. This is extremely important: transformation allows for comprehensive understanding of an individual gene's function (Busov et al. 2005). This high transformability allows for generation of large mutant poplars populations for gene discovery (aka, mutagenesis approaches). Mutagenesis through transformation is a preferred method in plants because the transformed DNA (T-DNA) serves as a tag allowing for facile positioning of the lesion in the genome.

Mutagenesis approaches typically result in two types of mutants – loss-of-function (LF) and gain-of-function (GF). LF results from disruption of a gene-reading frame often by T-DNA insertion. These LF mutations are recessive and require rounds of selfing to generate a progeny homozygous for the lesion that reveal the mutations effect. This makes LF impractical to study trees due to their long generation cycles (flowering occurs after many growing seasons). LF mutations are also problematic in plants due to the high level of gene redundancy observed in most plant genomes (Kondou, Higuchi, and Matsui 2010). This is especially problematic in poplars, which have experienced a recent whole-genome duplication (Kaul et al. 2000, Tuskan et al. 2006). Fortunately, these issues can often be circumvented using GF mutagenesis.

Activation tagging (AT) is one approach to GF mutagenesis that introduces T-DNAs containing known, strong enhancers located near to a boarder of the activation tagging vector (ATV). Thus, random genome insertion with the ATV by *Agrobacterium*-mediated transformation serves a dual purpose: (1) genome placement and (2) induced proximal gene transcription. The promoter's activity can operate more than 10kb from the insertion point to produce a GF phenotype observable in $T_0$ (e.g., the primary transformant) plants (Kondou, Higuchi, and Matsui 2010, Weigel et al. 2000).

In 2003, AT was first successfully used with poplars: within the pilot population a *Populus* GA2ox (GIBERRELLIN 2-OXIDASE) gene was discovered and characterized (Busov et al. 2003b). Subsequently, a number of other important *Populus* genes have been discovered and characterized using this method (Yordanov et al. 2014, Dash et al. 2017, Plett et al. 2010) demonstrating the feasibility for this approach in functional gene discovery.

The full-length complementary DNA overexpression (FOX) system is another GF mutagenesis approach (Ichikawa et al. 2006, Kondou, Higuchi, and Matsui 2010). The system uses *en block* transformation of a normalized full-length complementary DNA (fl-cDNA) library, directionally cloned between the strong 35S promoter and a terminator into transgenic plants (Carninci et al. 1996, Seki et al. 1998).

## 1.3 Appealing Features of the FOX System GF Mutagenesis Approach

First and foremost, the rate of mutant discovery of the FOX system is extremely high: using *Arabidopsis,* mutation rates range between ~10% and ~17% for the FOX approach (Ichikawa et al. 2006, Nakamura et al. 2007) compared to ~1% using AT (Weigel et al. 2000). Multiple poplar AT studies had similar results, displaying mutation rates of ~1.5% (Busov et al. 2003b, Busov et al. 2011). Furthermore, fl-cDNA libraries are specific to gene expression profiles, which are influenced by spatial, temporal and environmental cues (Seki, Narusaka, Kamiya, et al. 2002, Seki and Shinozaki 2009). Thus, specificity of RNA extraction theoretically enriches a FOX population for genes specific to a particular process. Therefore, the system not only increase the overall mutation rate but also the instances of finding genes that affect a trait of interest. Combined, these two factors elevate the economic feasibility of the FOX system.

FOX system greatly simplify the process of relating a gene to the observed GF phenotype in multiple ways. (1) The FOX system eliminates some ambiguities associated with cloning the causative genes using other methods like AT. For example, insertion of the ATV in a gene rich region can result in activation of several genes: these instances require expression

study of multiple genes making isolation of the causative more difficult. Furthermore, insertions in intron sequence as well as near genes prone to alternative splicing requires significant cloning work to identify the exact transcript that causes the phenotype. These difficulties do not exist in the FOX system as it relies on the introduction of already processed cDNA cloned into a predefined promoter/terminator context. The main difficulty of the FOX system arises with multiple insertions within a single line. However, *Agrobacterium*-mediated transformation typically generates 1-2 insertions within a single line (Gelvin 2012), thus there is a low level of complexity for determining the causative genes identity. (2) Cloning the culprit genes is also simpler using the FOX system: T-DNA promoter and terminator sequences flank the fl-cDNA and provide primer anchoring sites allowing for direct isolation of an inserted gene. AT relies on PCR with degenerate primers and/or ligation of adaptors, which may prove challenging in certain instances (Kondou, Higuchi, and Matsui 2010, Weigel et al. 2000, Ichikawa et al. 2006). (3) While AT is limited to studying endogenous genes, the FOX system can employ a transformable species to study FOX library generated from an entirely different species. This has been demonstrated multiple times (Kondou et al. 2009, Nakamura et al. 2007, Himuro et al. 2011, Higuchi-Takeuchi, Mori, and Matsui 2013), often using *Arabidopsis* to study rice fl-cDNA. Discovery of BROAD SPECTRUM RESISTANCE 1 (BSR1) from heterologous riceFOX *Arabidopsis* studies had real world application for development of biotechnology. Overexpression of BSR1 in the *Arabidopsis* plants generated a plant resistant to bacterial and fungal infections; subsequent overexpression in rice resulted in the similar phenotype (Dubouzet et al. 2011).

## 1.4 Regulation of Secondary Woody Growth

Secondary growth (aka woody growth) is the production of vascular tissues with cell walls that have secondary wall thickening. The tissues that arise because of secondary growth form wood, which as discussed earlier, largely defines the environmental and economic significance of trees. Thus, understanding the molecular mechanisms that affect wood biomass productivity and quality are of significant interest.

Secondary growth occurs in many plant taxa, including the model plant *Arabidopsis* but is short lived or a result of various types of treatments like decapitation, weight-induction and exogenous application of auxin (Levyadun 1994, Ko et al. 2004). Conversely, secondary growth occurs naturally (and in exaggeration) in trees and shrubs but these organisms are often difficult to use for molecular dissection. Thus, limited knowledge exists concerning the molecular mechanisms underlying secondary growth (Liu, Filkov, and Groover 2014). Nevertheless, significant progress has been made in the last years (reviewed in Zhang, Nieminen, et al. (2014) and Shi et al. (2017)). Secondary growth - like many other processes in plants - originates from meristem tissue, specifically vascular cambium. In many trees and shrubs vascular cambium is bifacial, meaning produces phloem to the outside and xylem to the inside of the stem trunk. Cambium cells actively divide and the active division zone is readily discernible by the size and shape of the undifferentiated cells. This cambial zone (CZ) is comprised of 6-8 cell files. The current progress for understanding the CZ regulatory mechanism involves a suit of various hormones and transcription factors (See Bhalerao and Fischer (2017), Ruzicka et al. (2015), and Du and Groover (2010) for extensive reviews).

Woody tissue development does not stop at the CZ: as the cells displace, they undergo expansion, differentiation, secondary cell wall (SCW) deposition and in case of xylem, programmed cell death (PCD). SCW and PCD are related processes that significantly affect woody biomass yield and quality. These determine the secondary cell wall composition that defines structural and mechanical properties of woody tissues (Li, Lu, and Chiang 2006). The major constitutes of cell wall are lignin, cellulose, and hemicellulose, which comprise 95% of woody dry weight biomass. Genes regulating SCW and PCD involve cell wall biosynthesis enzymes, transcription factors and intercellular cross talk genes (Zhang, Nieminen, et al. 2014, Ruzicka et al. 2015). Because these processes can significantly affect woody biomass yield and quality, the molecular controls regulating the sequence of progression is of substantial interest. Although mechanisms governing CZ, SCW and PCD are well studied, the larger understanding of these mechanisms and biosynthetic pathways is still limited.

## 1.5 Hypotheses & Objectives

To date, the FOX system has been only used in *Arabidopsis* (Dubouzet et al. 2011, Ichikawa et al. 2006, Fujita et al. 2007, Nakamura et al. 2007, Kondou et al. 2009) and *Lotus corniculatus* (bird's-eye trefoil) (Himuro et al. 2011). Given the limited number of species used with the FOX system, it is unclear if high rates of mutant discovery occur with other species. Furthermore, the use of the system for identification of genes specific to a process of interest has to date not been investigated. Our current study determines the feasibility of the FOS system for studying secondary growth in poplars.

Hypothesizes for our experiment:

1. Using model poplars with the FOX system will generate a transformant population with a high mutation rate.

2. RNAs extracted from succulent xylem to develop the fl-cDNA library will enrich the FOX poplars for mutants affected in traits linked to xylem development.

Objectives of study:

1. Implement the FOX system in poplar to study the process of xylem development

2. Determine basic parameters of how the system works in poplar

3. Validate the gene discoveries through a recapitulation process

# 2 Methods & Materials

## 2.1 Overview of Experiment

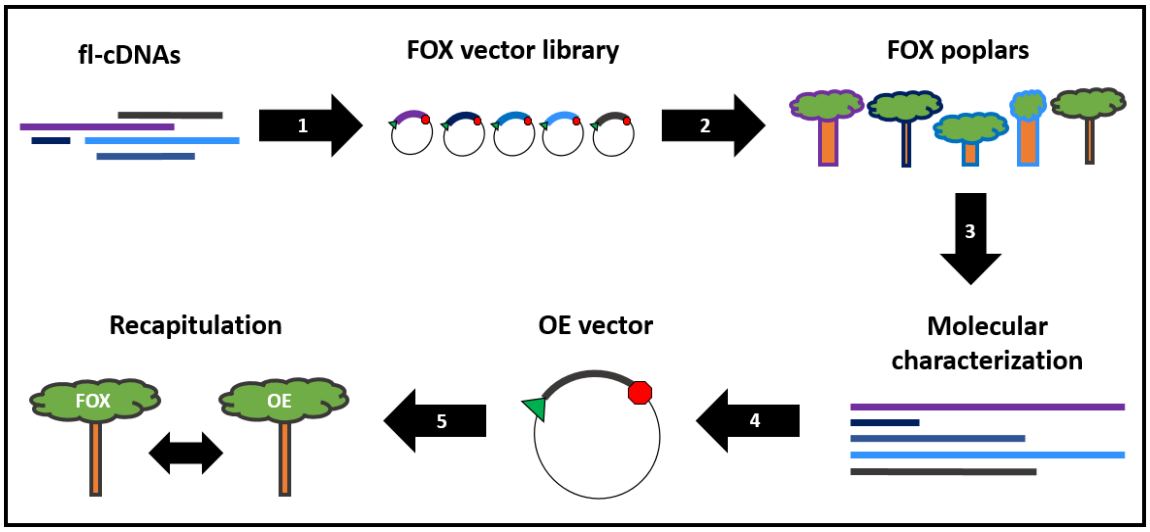


**Figure 2.1:** An overview of the experiment. RNA templates extracted from succulent xylem tissue were reverse transcribed generating the fl-cDNAs. (1) Individual fl-cDNAs were cloned independently and directionally within a FOX vector. (2) Using *Agrobacterium*, Wild type (wt) 717 poplars were transformed generating a population of FOX poplars. (3) FOX poplars with significantly distinctive phenotypes determined through screening. Fl-cDNAs configuring significant phenotypes were isolated and characterized with cloning and sequencing. To validate the FOX system, (4) a characterized fl-cDNA was directionally cloned into an overexpression (OE) vector and (5) using Agrobacterium was used to generate GF mutants. Phenotypes of FOX and OE lines were compared to determine effectiveness of the FOX system for poplar mutagenesis.

## 2.2 The FOX Poplar Library

### 2.2.1 A Xylem Specific FOX Library

Our intentions were to determine if the FOX system could be used to study genes associated with xylem development processes. To test this, we generated a collection of fl-cDNAs using succulent xylem tissue. Tissues were collected from an actively growing, approximately 15 year old aspen (*Populus tremuloides*) tree growing near the MTU campus using the method described in (Lin et al. 2014). We extracted total RNA using the

modified RNA extraction protocol (C.4). Bio S&T Inc. (Quebec, Canada) performed full transcript reverse transcription, amplification and normalization of fl-cDNAs. Proceeding this, the individual (fl)-cDNAs were cloned into the FOX vector pART277 (Fig. A.3) generating the FOX vector library.

### 2.2.2 FOX System Mutagenesis of Poplars

The FOX vector library was subsequently used for mutagenesis of the wt 717 poplar. First, D1H10B $T1^R$ E.coli were transformed with FOX library using heat shock protocol (E.1). D1H10B $T1^R$ transformants were grown on liquid LB (miller) media (F.2) with kanamycin (F.5) to select for presence of pART277 plant binary vector containing the kanamycin resistance gene. After growth period, the fl-cDNA:pART277 plant binary vector was extracted using QIAGEN maxiprep protocol (C.6). Glycerol Stock solutions of the transformed D1H10B $T1^R$ E.coli library was created using the protocol listed (E.3).

Next, 1µl of the extracted fl-cDNA:pART277 library was used to electrotransform Agl-1 *Agrobacterium* (Weigel 2002) (repeated 5 times). The electrotransformants were plated on LB (leonix) media (F.4) containing 50mg/L Rifampicin (F.6) and 100mg/L Spectinomycin (F.7). This generated 20 Petri plates (15cm diameter) containing approximately 1 million colonies. After a growth period of 48 hours all colonies were resuspended in 2 ml 50% glycerol per plate, and the entire bacterial library was collected in one 50ml tube and vortexed. A 0.5 ml aliquot from the library inoculated 100ml of liquid LB (leonix) (F3).

Finally, wt 717 hybrid poplars were transformed with the FOX library using the *Agrobacterium* transformation protocol (E.4). Approximately 100 putative transgenics, transformed with FOX library clones were PCR-verified for the presence of the nptII

selectable marker (Table B.1). The phenotypic subset of plants were analyzed for their respective transgene expression using qRT-PCR (C.10).

## 2.3 GF Recapitulation Poplars

As the FOX system had not been used with poplars, we needed to determine if the FOX phenotypes were due to GF mutation. To validate the FOX phenotypes, we selected a mutant FOX line for recapitulation using gateway OE protocol.

The cDNA used to generate the recapitulation constructs was amplified using B1 Pro35s and reverse B2 ocsCZ primers with modified B1 and B2 tails (respectively) (Table B.1 and Fig. B.2.1 and B.2.2) and the FOX plant gDNA (C.3). The BP clonase II protocol (D.3) was used to insert the amplified products into pDonr221 vector (Fig. A.4).

The reaction was transformed into competent *D1H10B T1$^R$ E.coli* using the heat shock protocol (E.1). Successfully transformed colonies inoculated 5ml of liquid LB (miller) media (F.2) containing 50mg/L kanamycin (F.5). Bacterial cultures were grown overnight at 37$^o$C and constant agitation and plasmid DNA extracted using the QIAGEN miniprep protocol (C.5). The presence of fl-cDNA confirmed using the restriction digestion protocol (D.1). DNA fragment size was predicted using ApE software.

The fl-cDNA were transferred from the pDonr vector into the pK7WG2 binary vector using the LR clonase protocol (D.4). The reaction was transformed into *D1H10B T1$^R$ E.coli* competent cells using heat shock (E.1). Selection of successfully transferred and transformed cells was as described above for the BP reaction with the exception of spectinomycin (50mg/L) used for selection media.

## 2.4 Phenotypic Analysis

Significance of the FOX lines was determined by screening each for a battery of traits. Three clonal replicates of each independent transgenic line, verified for the presence of nptII selectable marker (Table B.1) were grown under greenhouse conditions for three months. Each plant was measured for the following traits: height (cm), number of internodes, diameter at base (mm), diameter at 20 internode (mm), dry weight stem base (dw stem base) (g), green stem density (den-g) ($g/cm^3$), dry stem density (den-d) ($g/cm^3$), moisture content percentage (MC%), dry weight whole stem (dw whole stem) (g), dry weight leaves (dw leaves) (g) and cell wall content for cellulose, hemicellulose, and lignin (mass-to-charge ratio: m/z).

The den-g measurements were determined using stem base cutting. Mass of the cutting was recorded (g). The cutting was placed in a graduated cylinder to determine water displacement (ml). The density was determined by dividing the recorded mass by the volume.

The den-d measurements were determined using a similar manner to den-g: the difference between these measurement types was that the stem cuttings dried with the oven before taking measurements.

The moisture content percentage was determined by looking at the percent difference den-d and den-g measurements.

Cell wall content was determined with pyrolysis molecular-beam mass spectrometry analysis (PyMBMS): for further detail see Zhang, Novaes, et al. (2014).

Each line compared to wt 717 using a "student's" t-test (G.1).

# 3 Results

## 3.1 Screen under Greenhouse Conditions Identifies many Phenotypic Lines

Approximately 100 FOX lines, validated for the presence of the transgene were screened for changes in several traits (Table 3.1). We considered a FOX line to be a mutant as long as one trait displayed a significant p-value of less than 0.01. For these lines, all other traits significantly different from wt at p-values between 0 and 0.05 were also recorded (Table 3.1).

We found 20 of the 113 (17.7%) FOX poplars were significantly different from wt 717. We referred to these as mutant lines (Table 3.1). A majority of the mutant lines (16 of the 20) had multiple significantly altered traits: on average, approximately 4 were affected in a given line (Table 3.1). Many of the measured traits showed trends of predominant decrease or increase among the mutant lines (Fig. 3.1). For example, height, internode number, leaf dry weight and cellulose content decreased in more than half of the mutant lines, while change of lignin and percent moisture content showed opposite tendencies (Fig. 3.1). Traits measurements that showed decrease were more prevalent among the mutant lines (Fig. 3.1).

**Table 3.1:** Mutant poplar FOX lines. P-values determined using a Student t-test (unpaired, unequal variance, n>=3). A line was considered mutant if at least one trait was significantly different at P<0.01. Traits that were significantly different at P<0.05 in these same lines are also listed. See materials and methods for details about the growth conditions and traits' measurements. C5 - cellulose, C6 - hemicellulose, Den-D - density dry weight, Den-G - Density green weight, DW- dry weight, MC% - moisture content percentage, 20th - 20th internode.

| **P-values** | | |
|---|---|---|
| **FOX ID** | **< 0.01** | **< 0.05** |
| ***1F1-2*** | C6 | DW Whole Stem, Height, Internodes |
| ***1F1-3*** | C5, Height, MC% | C6, Diameter Base, Den-D, DW leaves, DW Stem Base, DW Whole Stem, Internode, Diameter 20th |
| ***1F1-5*** | C6 | Den-D, DW Stem Base, DW Whole Stem, Height, Internodes, Lignin, MC% |
| ***1F2-4*** | C6, Lignin | C5, DW Stem Base, DW Whole Stem, Height, Internodes, MC% |
| ***1F3-2*** | Lignin | C5 |
| ***1F3-4*** | C6, Diameter 20th | Den-D, DW Stem Base, DW Whole Stem, Height, Lignin, MC% |
| ***1F3-9*** | MC% | DW Whole Stem, Height, Internodes, Lignin |
| ***1F43-3*** | MC% | C6, DW Whole Stem, Lignin |
| ***1F47-4*** | C5, MC% | Height, Lignin |
| ***2F1-1*** | DW Leaves, Height, Internodes | Den-D |
| ***2F6-5*** | C5 | |
| ***2F58-1*** | Lignin | |
| ***3F10-6*** | Den-G | MC% |
| ***3F10-7*** | Den-G | C6 |
| ***3F10-8*** | Lignin | MC% |
| ***3F12-7*** | Height | DW Leaves, Internodes |
| ***3F16-5*** | C5 | DW Leaves |
| ***3F16-6*** | DW, Leaves, DW Whole Stem Height, Internodes, Diameter 20th | |
| ***3F17-7*** | Lignin | |
| ***3F90-4*** | C5 | |

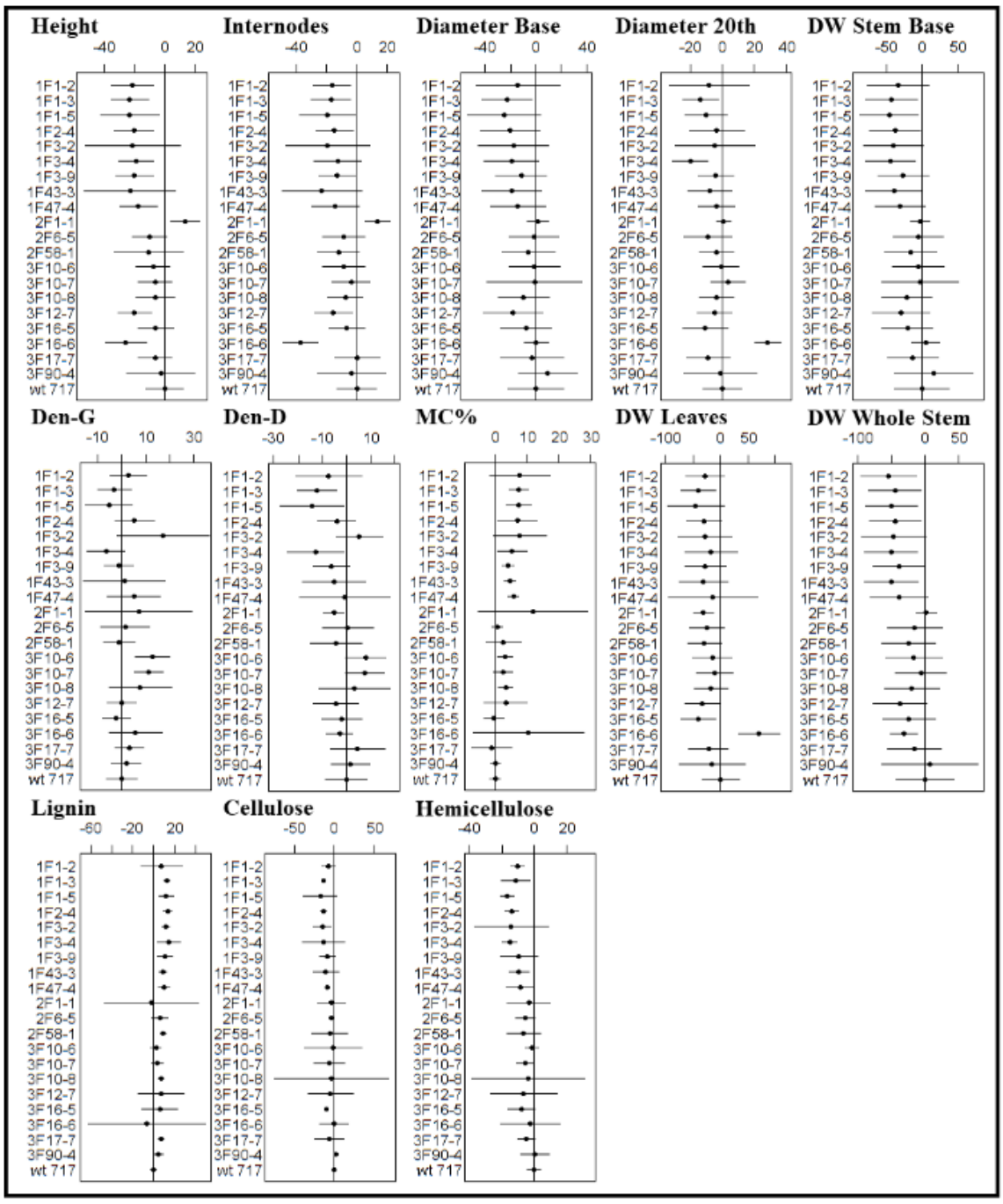


**Figure 3.1:** Traits' changes of mutant poplar lines. The confidence intervals are expressed as percent change from the wt 717 measurements. The x-axis represent the percent change. The y-axis indicate the genotype. A confidence interval for a trait that does not cross the 0% line is statistically distinct from wt 717 and is a phenotypic attribute of the FOX line (see Table 1 and text section G.3). C5 - cellulose, C6 - hemicellulose, Den-D - density dry weight, Den-G - Density green weight, DW-dry weight, MC – moisture content percentage, 20th - 20th internode.

## 3.2 Mutant Lines Predominantly Affected in Cell Wall Characteristics

We observed a significant variability with respect to the types of traits affected in the different mutant lines. Most prominently, 16 of the 20 mutant lines displayed significant differences from the wt 717 in stem cell wall composition (lignin, cellulose, and/or hemicellulose content) (Table 3.1 and Fig. 3.1). Using chi-square test, we found a highly significant enrichment for affected cell wall trait within the mutant FOX lines (Fig. 3.2). This outcome is consistent with the RNA source tissue used to generation the fl-cDNAs (e.g., succulent xylem). The enrichment of mutants affected in cell wall characteristics, suggests that the mutant phenotypes result from overexpression of genes involved in cell wall biosynthesis. Interestingly and unexpectedly, traits linked to developing xylem (*i.e.* stem diameter and density) were significantly underrepresented (Fig. 3.2). This suggests the tissue sampling uncovered a specific stage and/or a process that dominated xylem development.

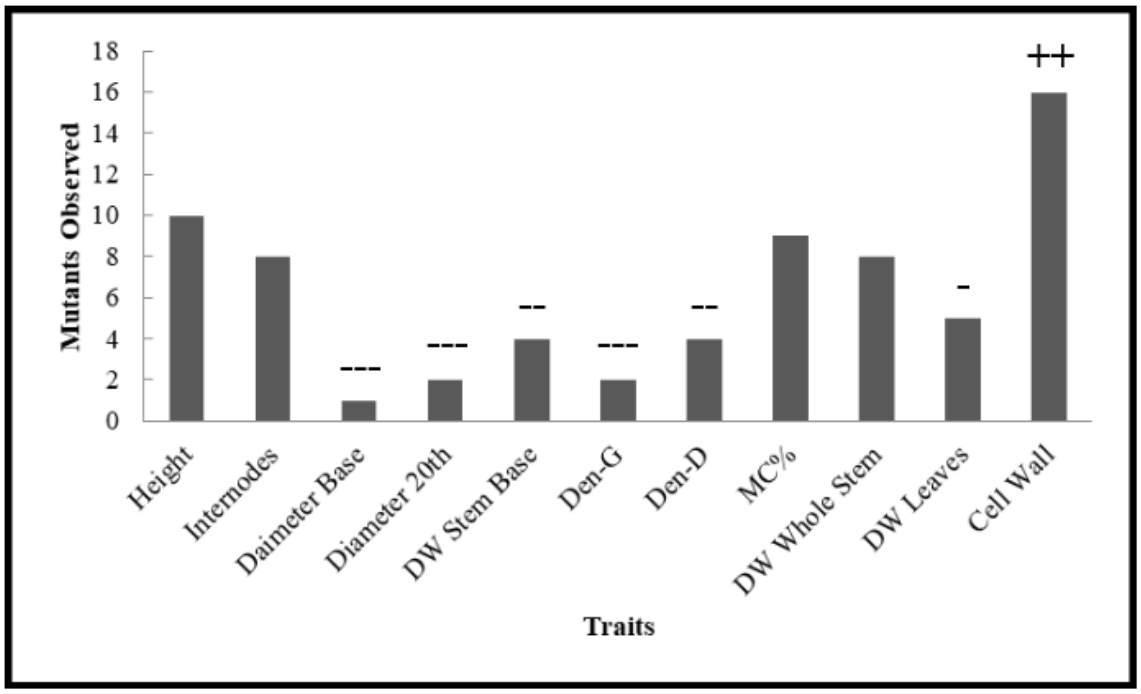


**Figure 3.2:** Affected traits are significantly over- and under-represented among the mutant FOX lines. Along the X-axis are measured traits. Along the Y-axis is the number of mutant line demonstrating significant difference from wt 717. P-values determined using a chi square test (unpaired, unequal variance, p=0.5, n=20, E=10, DF = 1). The '+' symbol indicates an overrepresented trait. The '-' symbol indicates an underrepresented trait. One, two or three of the '+/-' symbols indicate significance levels of $P<0.05$, 0.01 and 0.001, respectively. Den-D - density dry weight, Den-G - Density green weight, DW - dry weight, MC% - moisture content, 20th - 20th internode.

## 3.3 Molecular Characterization of FOX lines

To identify the genes underpinning the mutant phenotypes we PCR amplified the fl-cDNAs in all 20 mutant lines using a standard primer set designed to anneal to the 3' end of the 35S promoter and 5' end of the OCS terminator (Table B.1 and Fig. B.2.1 and B.2.2). Of the 20 phenotypic lines, there were 13 single and 7 double insertions as evidenced by the number of bands amplified (Fig 3.4). We observed no mutant line with three fl-cDNA insertions. Among the mutants, the average insertion per line was 1.35 (Fig 3.4).

Of the 27 fl-cDNAs identified in the mutant lines, 24 were sequenced (Table 3.2). The lines with double fl-cDNA insertions required agarose gel purification; purification result in low DNA concentrations that are unacceptable for the accurate sequencing. We attribute all unsequenced fl-cDNAs to this. Additionally, we sequenced 32 fl-cDNAs from non-phenotypic FOX lines (Table H.1).

## 3.4 Mutant FOX Lines Harbor fl-cDNAs Linked to Xylem and Cell Wall Development

Because of the relatively small number of genes/lines, we were unable to define a significantly enriched gene ontology (GO) categories. However, some of the FOX genes found in the mutant lines have a clear link to xylem development and particularly the cell wall biosynthesis. For example, the fl-cDNAs identified in 1FOX2-4.1, 1FOX3-9, 2FOX6-5 and 3FOX90-4 lines showed strong homology to MICROTUBULE ASSOCIATED PROTEIN 65-8 (MAP65-8), IRREGULAR XYLEM 9 (IRX9), MYB103 and FASCICLIN-LIKE ARABINOGLACTAN PROTEIN 17 PRECURSOR (FLA17) from *Arabidopsis* (respectively)(Table 3.2). MAP genes are involved in assembly of microtubule biopolymers and regulates cell wall structure between plant cell (Wasteneys 2002); IRX9 is a non-CLS (cellulose-synthase-like gene) involved in xylan biosynthesis (York and O'Neill 2008); MYB transcription factors have been found to regulate lignin biosynthesis (Ohman et al. 2013); FLA proteins have roles in wood formation in poplars (Wang et al. 2017). Consistently, cell wall compositions for 1FOX2-4, 1FOX3-9, 2FOX6-5 and 3FOX90-4 were all found to be significantly different from wt 717 (1FOX2-4: lignin, cellulose, and hemicellulose; 1FOX3-9: cellulose; 2FOX6-5: lignin; 3FOX90-4: lignin)

(Fig 3.1 and Table 3.1). These findings are consistent with the enrichment of mutant lines affected in cell wall composition (Fig 3.2).

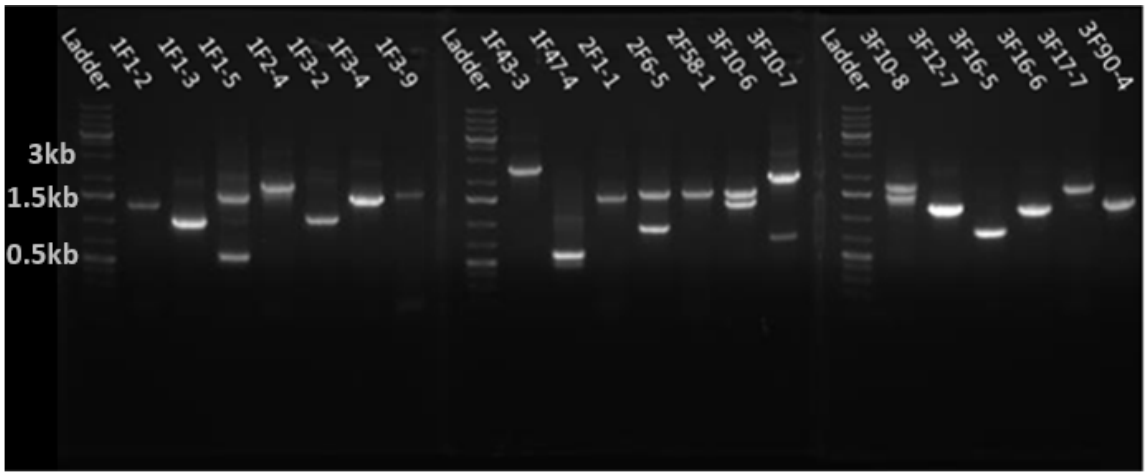


**Figure 3.3:** PCR amplification of the insertions in the mutant FOX lines. A GeneRuler 1kbp Plus DNA ladder used to determine sizes of fragments.

**Table 3.2:** Functional annotation of the fl-cDNAs identified from mutant lines. Lines with more than 1 insertion are indicated with the same line number but with the '.1' and '.2' extensions. E-values based on Basis Local Alignment Sequencing Tool (BLAST) analysis of gene against *P.trichocarpa* genome (continued on next page).

| FOX line | E-Value | Pt Gene ID | At Ortholog AGI | Gene Name/Description |
|---|---|---|---|---|
| ***1F1-2*** | 0 | Potri.002G104400 | AT2G22500 | DICARBOXYLATE CARRIER 1 (DIC1) |
| ***1F1-3*** | 1.9E-127 | Potri.001G242300 | AT5G59480 | HALOACID DEHALOGENASE LIKE HYDROLASE (HAD) |
| ***1F1-5.1*** | 8.2E-145 | Potri.002G070200 | AT1G21320 | Nucleic acid/nucleotide binding protein |
| ***1F2-4.1*** | 8.9E-132 | Potri.003G173300 | AT1G27920 | MICROTUBULE ASSOCIATED PROTEIN 65-8 (MAP65-8) |
| ***1F2-4.2*** | 6.8E-67 | Potri.015G036000 | AT3G17880 | HSP70 INTERACTING PROTEIN 2(HIP2) |
| ***1F3-2*** | 0 | Potri.005G033200 | AT3G05330 | TANGLED1 (TAN1) |
| ***1F3-4*** | 0 | Potri.001G029600 | AT5G13530 | KEEP ON GOING (KEG) |
| ***1F3-9*** | 0 | Potri.016G086400 | AT2G37090 | IRREGULAR XYLEM 9 (IRX9) |
| ***1F43-3*** | 0 | Potri.007G016100 | AT4G36210 | DUF726 |
| ***1F47-4.1*** | 1E-133 | Potri.013G013000 | AT1G56230 | DUF1399 |
| ***1F47-4.2*** | 2.4E-102 | Potri.005G101400 | AT1G20693 | HIGH MOBILITY GROUP B2 (HMGB2) |
| ***2F1-1*** | 0 | Potri.014G045100 | AT4G16780 | HOMEOBOX LEUCINE ZIPPER PROTEIN 4 (HAT4) |
| ***2F6-5.1*** | 1.3E-113 | Potri.003G132000 | AT1G63910 | MYB DOMAIN PROTEIN 103 (MYB103) |
| ***2F6-5.2*** | 2.4E-35 | Potri.002G160200 | AT2G45910 | U-box domain-containing protein kinase family protein |
| ***2F58-1*** | 5.4E-115 | Potri.002G216000 | AT1G54790 | GDSL-motif esterase |
| ***3F10-6.1*** | 0 | Potri.002G051400 | AT5G36740 | Acyl-CoA N-acyltransferase with RING/FYVE/PHD-type zinc finger protein |

| FOX line | E-Value | Pt Gene ID | At Ortholog AGI | Gene Name/Description |
|---|---|---|---|---|
| ***3F10-6.2*** | 2.4E-164 | Potri.002G067600 | AT1G21090 | Cupredoxin superfamily protein |
| ***3F10-7.1*** | 0 | Potri.006G279100 | AT4G31270 | HARBINGER TRANSPOSON DERIVED PROTEIN 2 (HDP2) |
| ***3F10-8.2*** | 4.5E-86 | Potri.013G086700 | AT5G36290 | Uncharacterized protein family (UPF0016) |
| ***3F12-7*** | 0 | Potri.018G047700 | AT2G26280 | CTC-INTERACTING DOMAIN 7 (CID7) |
| ***3F16-5*** | 2.1E-176 | Potri.004G210800 | AT2G28430 | C3HC4 type family protein |
| ***3F16-6*** | 3.5E-89 | Potri.009G010800 | AT2G28305 | LONELY GUY 1 (LOG1) |
| ***3F17-7*** | 8.9E-176 | Potri.008G020900 | AT3G54260 | TRICHOME BIREFRINGENCE-LIKE 36 (TBL36) |
| ***3F90-4*** | 0 | Potri.008G012400 | AT5G06390 | FASCICLIN-LIKE ARABINOGLACTAN PROTEIN 17(FLA17) |

## 3.5 fl-cDNA Upregulation

We validated fl-cDNA upregulation for a subset of FOX lines: both mutant and non-phenotypic lines were used (Tables 3.2 and H.1). Although, all fl-cDNA inserts were upregulated, there was a significant variation in the level of upregulation: approximately half of the lines showed expression increases up to 100-fold range. Interestingly, the other half showed huge upregulation levels, measuring into the thousands fold levels (Figure 3.4). The average upregulation level across all tested FOX lines was 1,423 fold greater that the wt 717 plant.

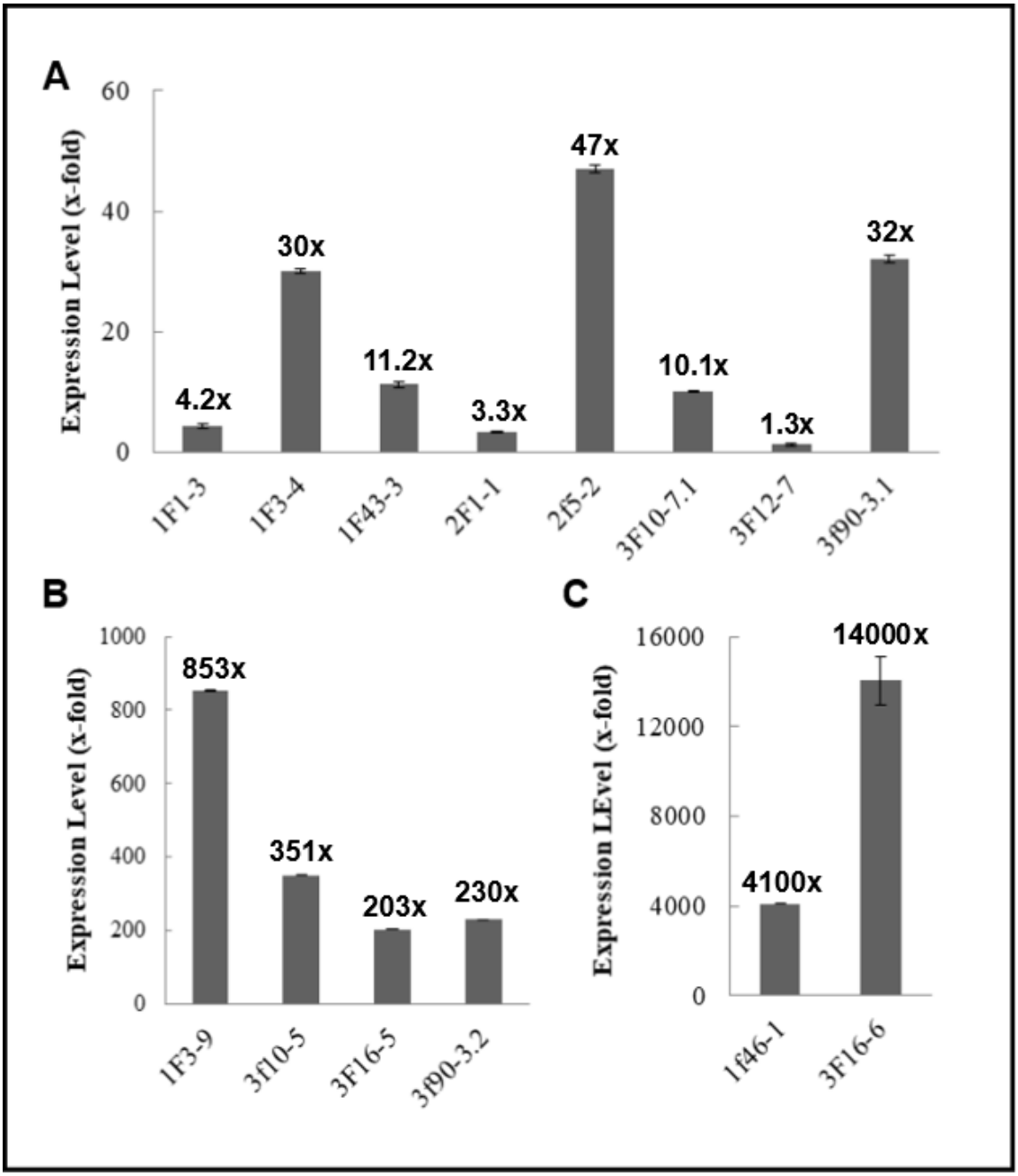


**Figure 3.4:** Validation of fl-cDNA upregulation in 14 different FOX lines. Overexpression tested in both phenotypic and non-phenotypic FOX poplar lines. A) Lines that showed upregulation up to 100 fold. B) Lines that showed overexpression levels greater than 100 and less than 1000 fold. C) Lines that showed overexpression levels greater than 1000 fold. 'F' indicates Mutant line; 'f' indicates non-phenotypic line.

## 3.6 *P.trichocarpa* Homologs to fl-cDNAs Expressed Predominantly in Xylem

Because we extracted RNA from succulent xylem, we expected the fl-cDNA *P.trichocarpa* homologs to be expressed predominantly in xylem tissues. Using recently published RNA-seq data gathered from multiple tissue types (Shi et al. 2017) and the 56 known fl-cDNAs sequences (Tables 3.2 and D.1) we interrogate the tissue-specificity (if any) of the recovered genes (Fig 3.5). Consistent with our expectations, we found the majority of fl-cDNA homologs had highest expression in xylem tissue.

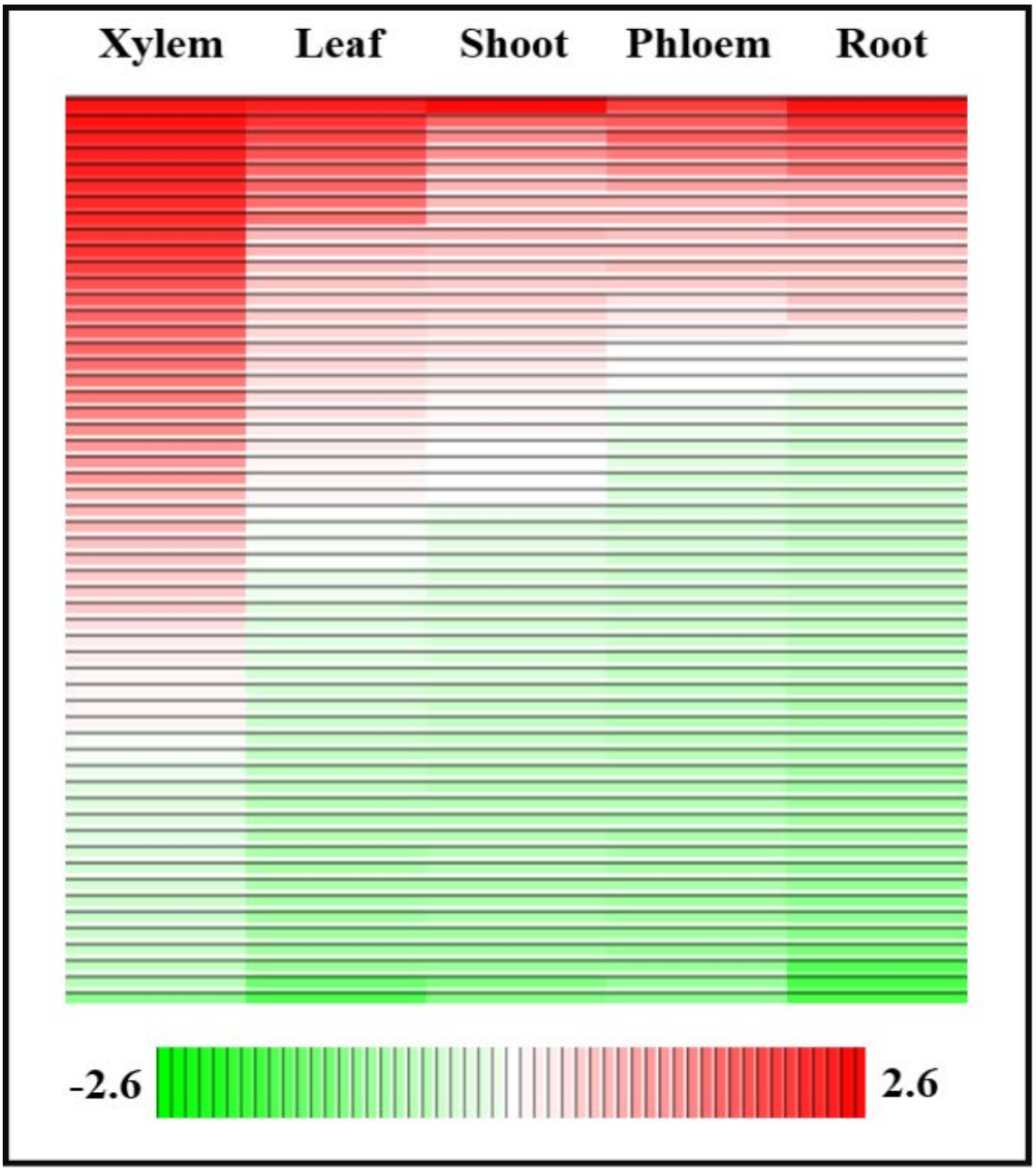


**Figure 3.5:** Tissue-specific expression of *P.trichocarpa* homologs of recovered fl-cDNAs. Expression estimates are based on published RNA-seq data by Shi et al. (2017). Z-scores were generated for each fl-cDNA based on the averages RNA expression results at each tissue (n=3). Each category was arranged from highest to lowest Z-score. A Z-score scale shows the range of values observed; the green color indicates a Z-score demonstrating a comparatively low expression for a gene at a particular tissue; the red color indicates a Z-score demonstrating a comparatively high expression for a gene at a particular tissue. Scale bar at the bottom indicates the expression ranges. Heat map image was generated using Netwalker 1.0 software.

## 3.7 Discovery of Line with Increased Xylem Proliferation

The mutant line, 3FOX16-6, displayed a phenotype of particular interest. Unlike other mutants, 3FOX16-6 was affected at the significant level of $P<0.01$ in five traits: height, internode number diameter at 20th internode, and dry weight of both leaf and whole stem (Table 3.1 and Fig. 3.1, 3.6, and 3.7). 3FOX16-6 also showed decreased apical dominance as evidenced by frequent occurrence of sylleptic branch proliferation (Fig. 3.7C).

Because of the significant increase in diameter, we studied the anatomy of stem and the tissue(s) that contribute to the observed diameter increases (Fig. 3.8). We found the xylem radial width to be nearly doubled (1.89x) and the single major contributing factor to increased stem girth of the 3FOX16-6 lines (Fig. 3.8B).

Significant changes to growth and development often impact cell wall structure (Du and Groover 2010). We observed no significant alteration to the three major cell wall constituents – lignin, cellulose and hemicellulose (Fig. 3.9).

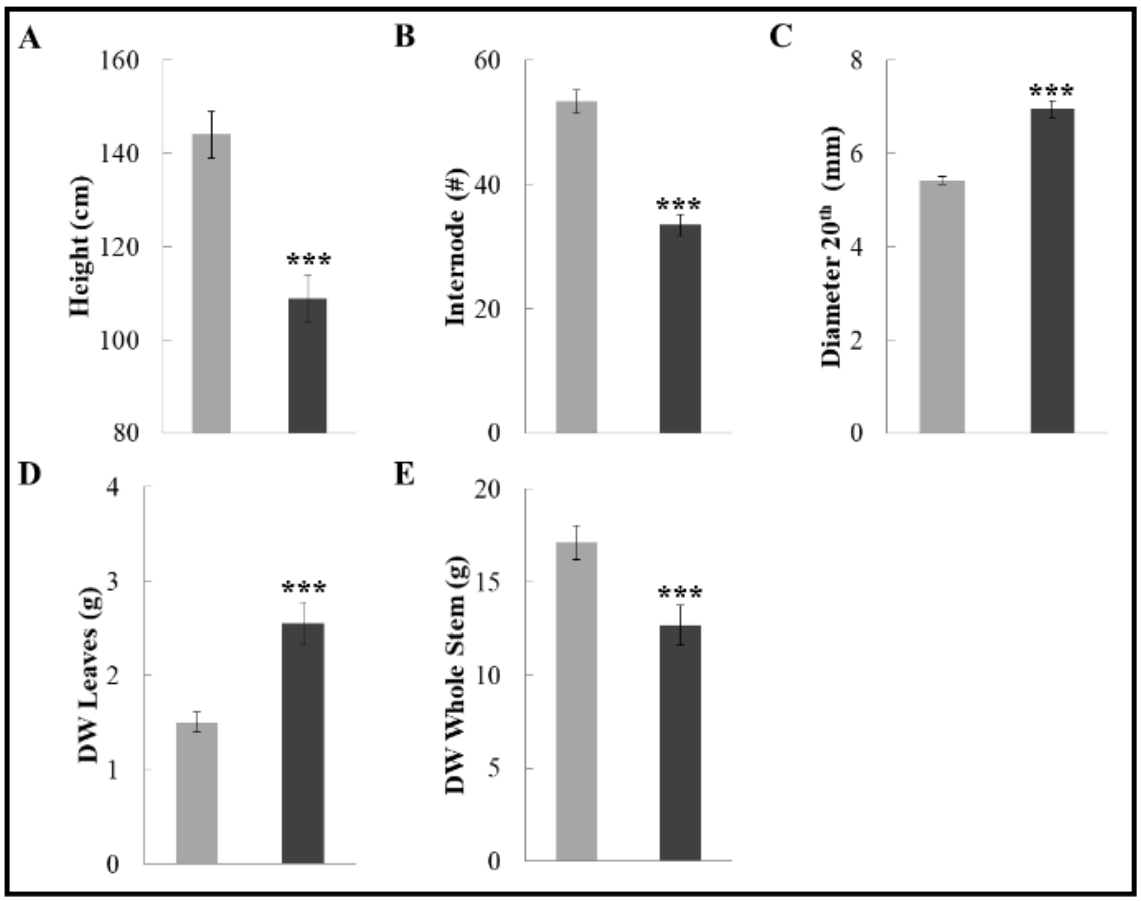


**Figure 3.6:** 3FOX16-6 mutant line shows a suite of phenotypic changes. Significance of the differences determined using a Student t-test (unpaired, unequal variance, n>=9). One, two or three of asterisks indicate significance levels at P<0.05, 0.01 and 0.001, respectively. Light and dark grey bars indicate wt 717 and 3FOX16-6 line, respectively. DW-dry weight, 20th - 20th internode.

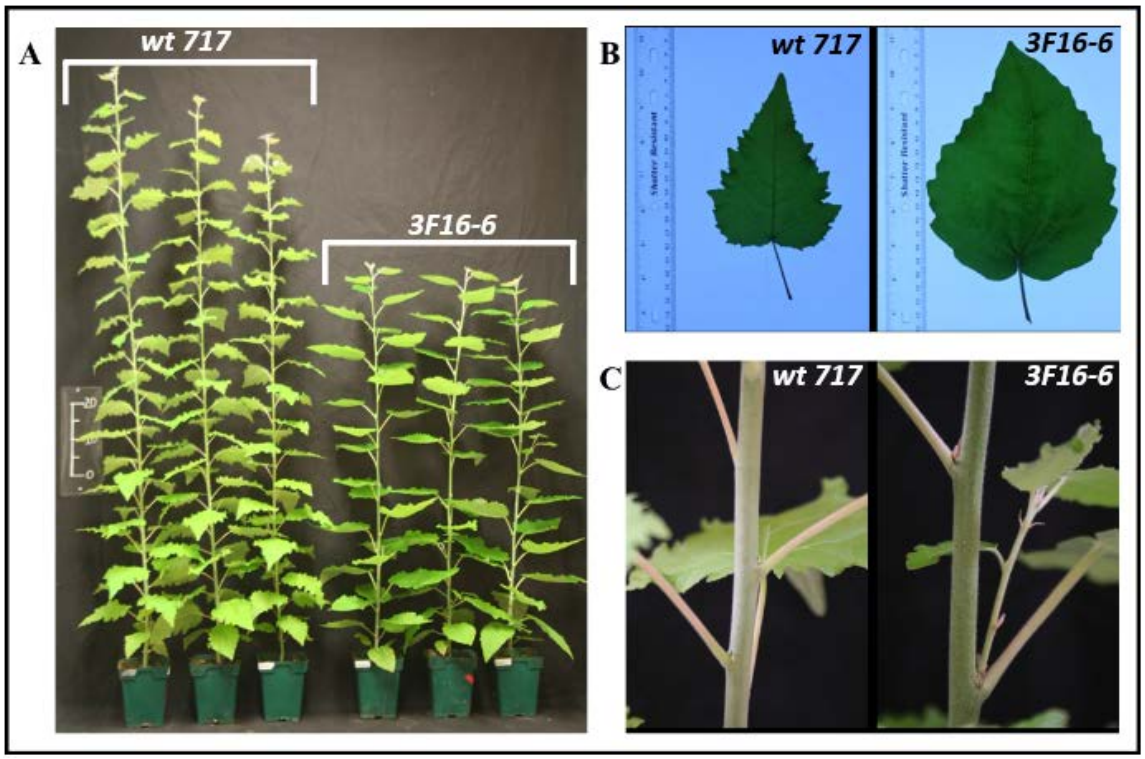


**Figure 3.7**: 3FOX16-6 phenotypic changes. A) Whole plant photographs: on left, three ramets of wt 717: on right, three ramets of 3FOX16-6 line. B) Representative fully developed leaves from the 15th internode: on left, wt 717: on right, 3FOX16-6. C) Sylleptic branch outgrowth in 3FOX16-6: on left, wt 717: on right, 3FOX16-6.

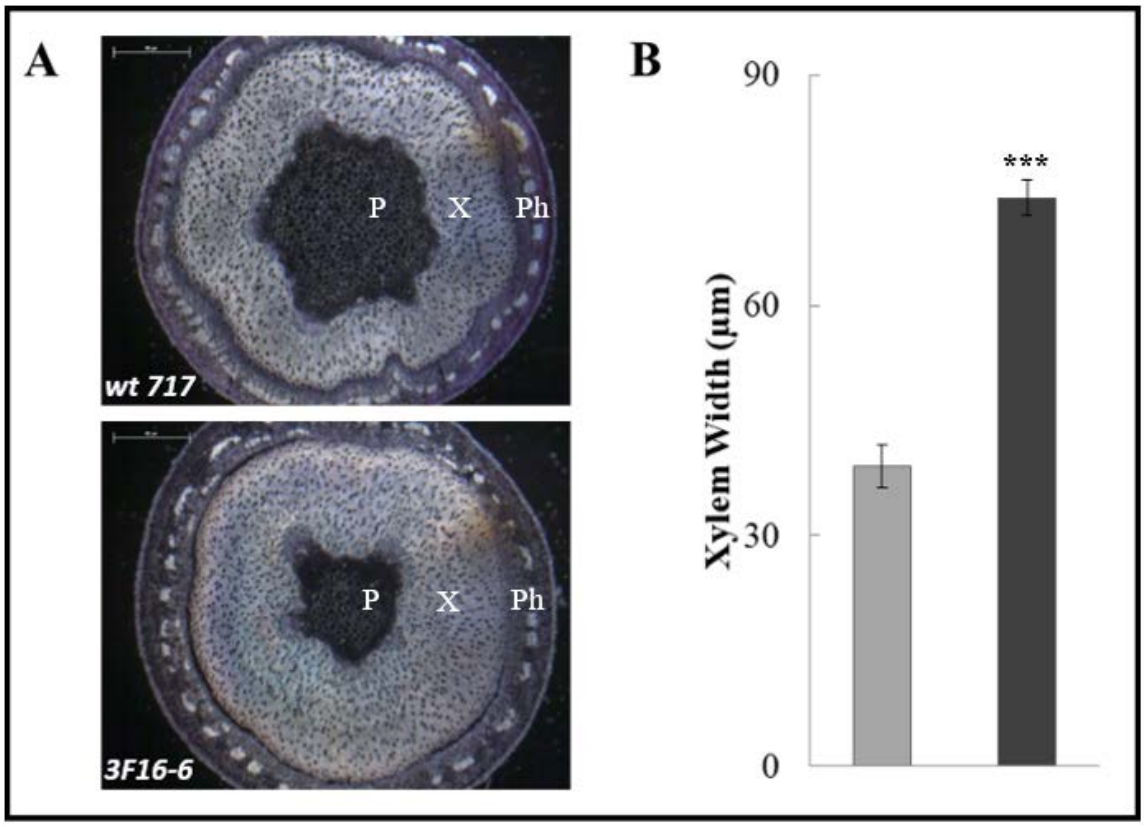


**Figure 3.8:** displays increased xylem proliferation. A) Transverse stem sections taken from the 15th internode. On top, wt 717: on bottom, 3FOX16-6. B) Xylem width; light and dark grey indicates wt 717and 3FOX16-6 lines; Significance of the differences were determined using a Student t-test (unpaired, unequal variance, n>=4). One, two or three asterisks indicate significances at P<0.05, 0.01 and 0.001, respectively. Scale bar = 50 µm. P - Pith, Ph - phloem, X - xylem.

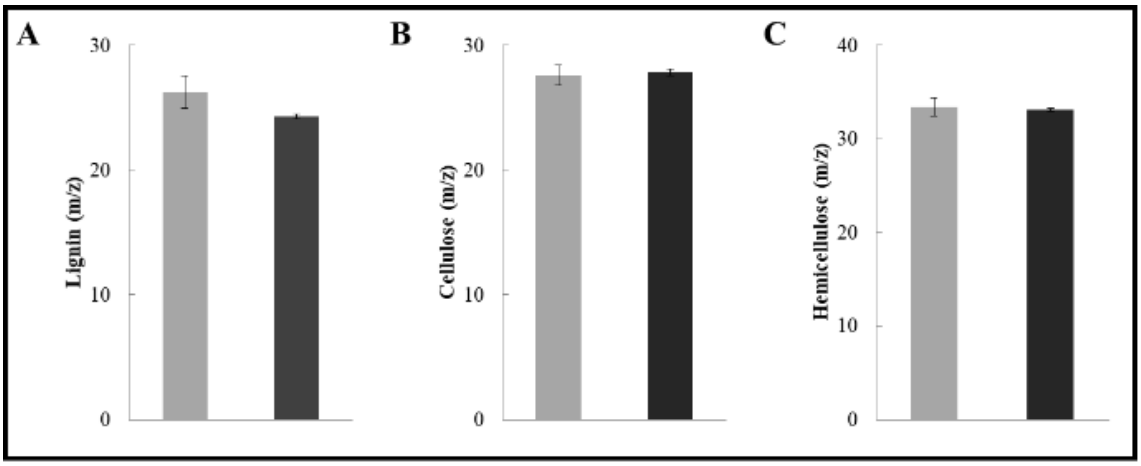


**Figure 3.9:** Cell wall composition in 3FOX16-6 is unchanged. Statistical significance was tested using a Student t-test (unpaired, unequal variance, n>=9). Light and dark grey bars indicate wt 717 and 3FOX16-6, respectively. A) Lignin. B) Cellulose. C) Hemicellulose. Measured using PyMBMS analysis. m/z - mass-to-charge ratio.

## 3.8 Upregulated fl-cDNA of 3FOX16-6 Shows Homology to LONELY GUY 1 (LOG1)

The sequence of the fl-cDNA upregulated (Fig 3.3) in 3FOX16-6 line showed highest sequence homology to LONELY GUY 1 (LOG1) from *Arabidopsis* and *P.trichocarpa* (Table 3.2). We therefore named the gene *PtaLOG1* (*Populus tremula X alba=Pta*). The LOG1 gene was initially characterized in rice, and found to encode an phosphoribohydrolase enzyme from the cytokinin biosynthetic pathway (Kurakawa et al. 2007).

Inactive cytokinins are synthesized by modifications to an adenine base of an adenosine-5'-(tri-, di-, mono-)phosphate by ISOPENTYL TRANSFERASE (IPT) (Sakakibara 2006). Initially, biological activation of cytokinin was thought to be regulated only through a two step conversion pathway requiring nucleotidase and nucleosidase for consecutive removal of inorganic phosphate and riboside groups, respectively (Sakakibara 2006) (Fig. 3.11A). The discovery of the LONELY GUY gene family revealed an alternative cytokinin

activation pathway where LOG can remove the phosphorylated riboside (ribosine-5'-(tri-,di-,mono-)phosphate) in a single step reaction (Fig. 3.11A) (Kurakawa et al. 2007).

## 3.9 LOG Genes Constitute a Small Family with Tissue-Specific Expression & Enzymatic Specificity

A small gene family found in Arabidopsis and poplars with 9 and 15 members, respectively, encodes these enzymes (Immanen et al. 2013, Tokunaga et al. 2012). The different family members show differential expression and condition-specific enzyme optimums; this is suggestive of an evolution of LOG genes with specific functions in plant development (Kuroha et al. 2009). We found *PtaLOG1* showed highest sequence homology to *PtLOG1a* which clusters in a clade containing *AtLOG1/3/4*, *PtLOG1/6/8d* (Fig. 3.10).

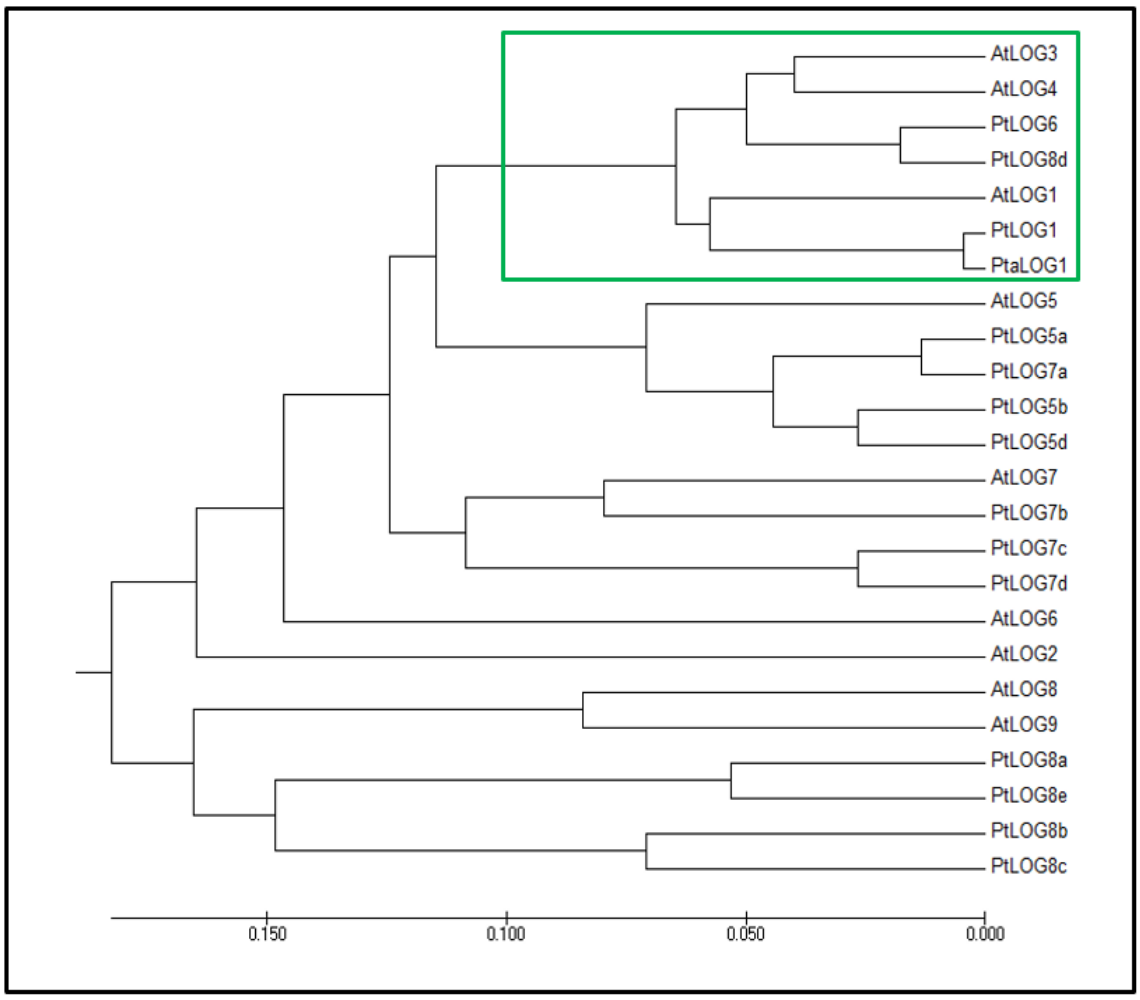


**Figure 3.10:** The evolutionary history was inferred using the UPGMA method (Sneath and Sokal 1973). The optimal tree with the sum of branch length = 2.04005468 is shown. The tree was drawn to scale, with branch lengths in the same units as those of the evolutionary distances used to infer the phylogenetic tree. The evolutionary distances were computed using the p-distance method (Thomas 2001). The analysis involved 24 amino acid sequences. All positions containing gaps and missing data were eliminated. There were 113 positions in the final dataset. *PtaLOG1* falls within a distinctive clade (outlined in green) containing the Arabidopsis homologs *AtLOG1/3/4* and poplar homologs *PtLOG1/6/8d*. *PtaLOG1* was most homologous to *PtLOG1*. Evolutionary analyses were conducted in MEGA7 (Kumar, Stecher, and Tamura 2016).

## 3.10 Active Cytokinins are Significantly Increased in 3FOX16-6 Mutant Line

To validate that *PtaLOG1* had biochemical function in cytokinin biosynthesis, we investigated the levels of multiple cytokinin precursors and active forms in 3FOX16-6 line and compared them to wt 717 plants. Stem and leaf tissues were used in the analysis. Indeed, consistent with a role of *PtaLOG1* in cytokinin activation, 3FOX16-6 plants showed significantly higher concentrations of iP within both stem and leaf tissues when compared to wt 717 plants (Fig. 3.11). The LOG substrate (iPRMP) also decreased significantly in stem tissues (Fig 3.11B).

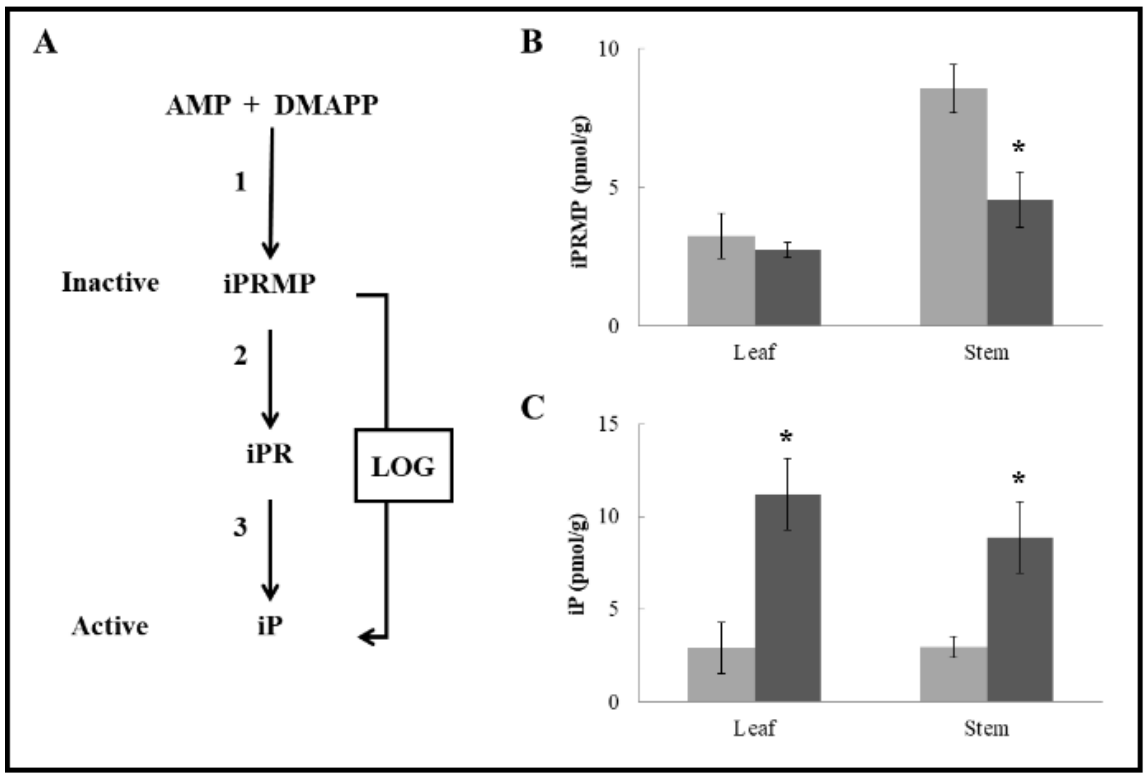


**Figure 3.11:** Significantly altered cytokinin concentrations of 3FOX16-6. A) The biosynthesis and activation pathway for the iP type of cytokinins; 1) ISOPENTYL TRANSFERASE (IPT) modifies the adenine base of AMP generating iPRMP; 2) first step in the two step pathway: nucleotidase removal of inorganic phosphate from iPRMP generates iPR; 3) second step in the two step pathway: nucleosidase removal of riboside group from iPR generates iP. LOG gene activity of cytokinin nucleoside 5-monophosphate phosphoribohydrolase directly convert iPRMP to iP in a single step (Kurakawa et al. 2007, Sakakibara 2006). B) iPRMP concentrations from leaf and stem samples. C) iP concentrations from leaf and stem samples. Significance determined with a Student t-test (unpaired, unequal variance, n=4). '*' indicates significance difference at $P<0.05$. Light and dark grey bars indicate wt 717 and 3FOX16-6, respectively AMP - adenosie monophosphate, DMAPP - dimethylallyl diphosphate, iP - isopentenyl adenine, iPR - iP riboside, iPRMP - isopentenyl adenosine monophosphate, LOG - LONELY GUY.

## 3.11 Highest *PtaLOG1* Expression in Xylem Tissues

Using the data from Shi et al. (2017), we studied the *PtLOG1* (the closest in homology to *PtaLOG1*) expression pattern. *PtLOG1* showed highest expression in xylem, vessel and phloem tissues: the highest expression of *PtLOG1* was in xylem tissue (Figure 3.12).

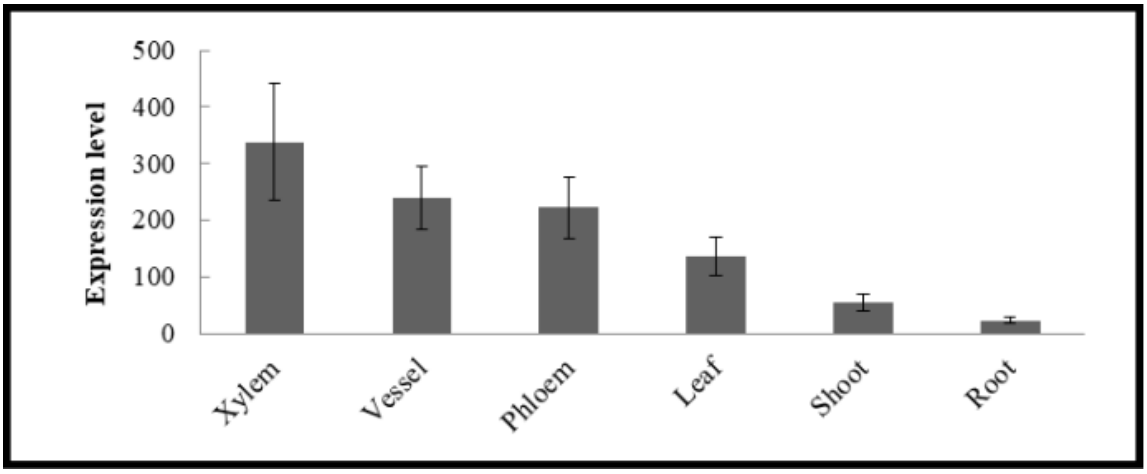


**Figure 3.12:** *PtLOG1* shows highest expression in xylem tissues. Expression quantified with published RNA-seq data (Shi et al., 2017). Error bars indicate standard deviation across three samples.

## 3.12 FOX *PtaLOG1* Phenotype Successfully Recapitulated

Cloning *PtaLOG1* into a separate overexpression construct was imperative to validating the results of this study for two reasons. First, recreating the 3FOX16-6 phenotype with another method using the same fl-cDNA demonstrates the *PtaLOG1* as the culprit. Second, recreation of a FOX phenotype in another method validates the FOX hunting method can be used in conjunction with *Populus tremula X alba* for GF gene analysis.

We recovered twelve independent *PtaLOG1* OE lines validated with transgene upregulation (Fig. 3.13). Our results demonstrated variability in *PtaLOG1* upregulation among the OE lines: we expected the OE lines with highest *PtaLOG1* expression would confer a comparable phenotype to 3FOX16-6 (Fig. 3.4c and 3.13). These predictions were

confirmed, three independent lines (OE15, OE11-2, and OE17-2) displayed significance for the same trait set that were unique to the 3FOX16-6 lines (Figure 3.14). In addition to the three completely recapitulated lines was a fourth line (OE17-1) displaying three of the recapitulated traits.

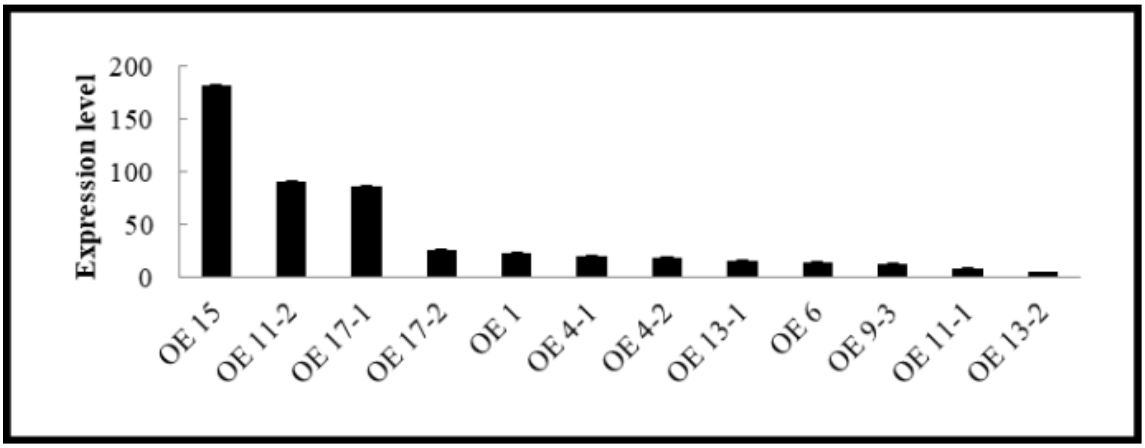


**Figure 3.13:** *PtaLOG1* expression levels of various recapitulation overexpression lines. Lines arranged based on *PtaLOG1* expression levels (high to low). OE - *PtaLOG1* overexpression line.

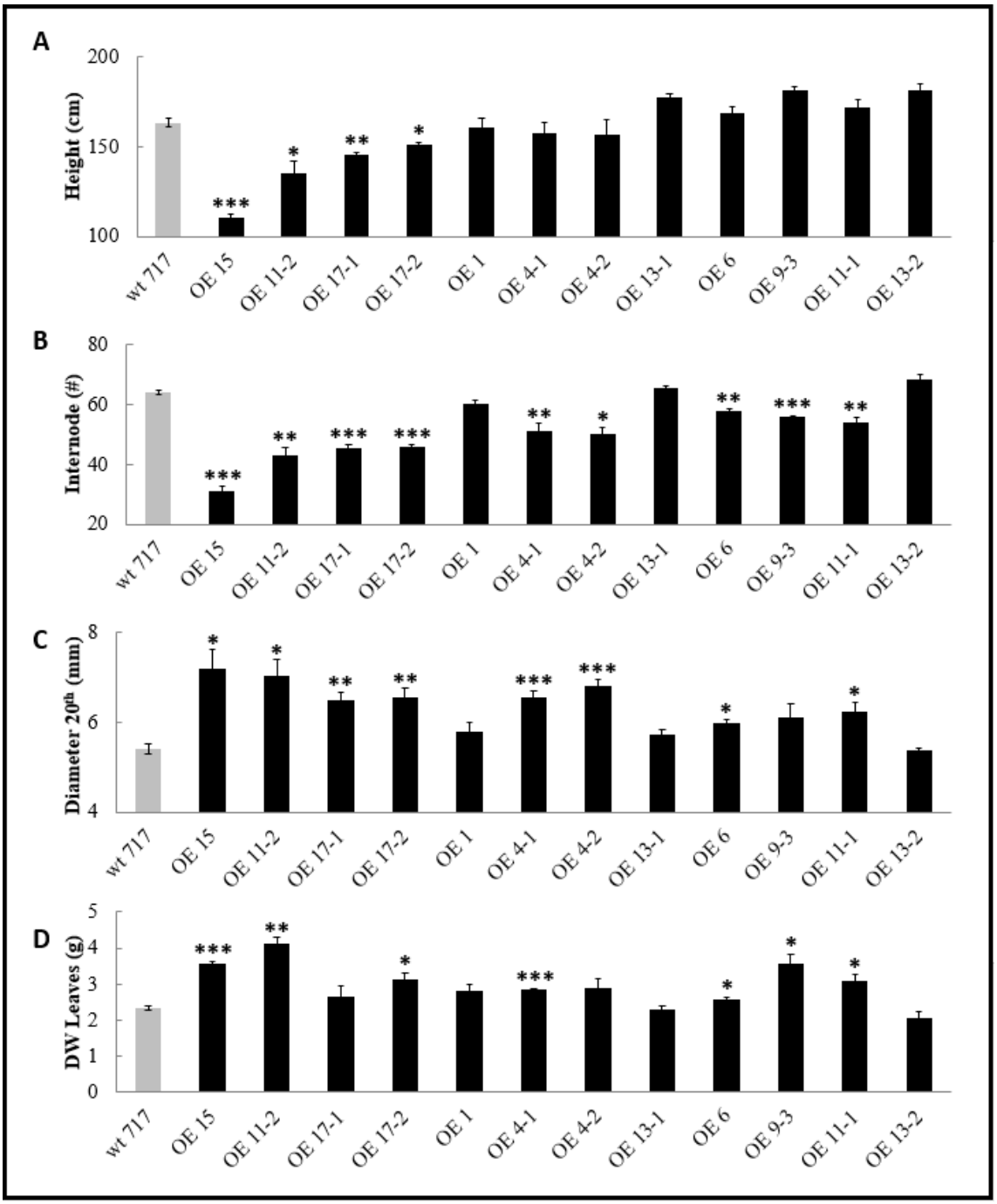


**Figure 3.14:** *PtaLOG1* Overexpression lines demonstrate complete and partial recapitulation. Significance of the differences determined using a Student t-test (unpaired, unequal variance, n>=3). One, two or three asterisks indicate significances at P<0.05, 0.01 and 0.001, respectively. DW - dry weight. 20th - 20th internode.

# 4 Discussion

## 4.1 Purpose of Experimentation

Using a pilot population of 113 independent lines, we examined the feasibility and efficiency of the FOX system in poplar for discovery genes controlling secondary woody growth, a process of major economic and environmental significance. We focused on the potential of this system for overcoming difficulties associated with applying traditional mutagenesis approaches to studying trees. Specifically, we were interested if the FOX system could increase the overall mutation rate and the frequency of mutants affected in a specific trait of interest: in this experiment wood formation.

## 4.2 FOX System Generates High Mutation Rates with Poplars

First, we determined the overall mutation rate. Screening for a battery of traits revealed a mutation rate of 17.7%, which was 12-fold increase to the mutation rates observed using activation tagging with poplars (~1.5% average) under greenhouse conditions (Busov et al. 2011, Busov et al. 2003a). However, this outcome was not unusual. In *Arabidopsis*, mutation rates using the FOX system, ranged between ~10% and ~17% (Ichikawa et al. 2006, Nakamura et al. 2007). Given our very stringent cut-off p-value used for determining the significance of the phenotypic changes in the mutant lines, there is possibility for the mutation rate to be even greater. The high mutation rate engendered by using the FOX system can significantly improve the efficiency and cost of gene discovery obtained through mutagenesis.

## 4.3 Enrichment for Mutants Affected in Cell Wall

In addition to mutation rate, the proportion of mutants affected in a particular trait of interest is another factor influencing efficiency and feasibility of mutagenesis. Because mutagenesis is by nature random, the affected genes and traits are also random and thus the proportion of mutants affected in a specific trait of interest are only a fraction of all mutants discovered. Gene expression is specific: generally, the spatial and temporal expression patterns for genes important to a specific process is highest during a traits development. Hypothetically, a FOX library derived from a pool of RNA closely linked to the trait of interest should have higher occurrence of fl-cDNAs corresponding to genes important for this trait. Such tissue-specific FOX libraries would thus have a higher probability of producing phenotypic changes in the specific trait under study (Seki, Narusaka, Ishida, et al. 2002, Seki, Narusaka, Kamiya, et al. 2002). We tested this hypothesis by a generating the FOX library from RNA derived from developing xylem – tissue that give rise to wood. We expected this to increase the frequency of mutants affected in wood formation relative to other traits/processes.

Several lines of evidence suggest that the FOX system does indeed increase the proportion of mutants affected in wood formation relative to other traits/processes. First and most importantly, the only trait that's frequency of occurrence was disproportionately and significantly increased relative to the other 10 measure traits was cell wall composition characteristics (e.g., cellulose, lignin and/or hemicellulose) (Fig 3.2). 80% of all the discovered mutants were significantly affected in at least one of these three main cell wall constituents. Because wood formation requires massive synthesis of secondary cell wall

structure, it is not surprising that genes involved in this synthesis are highly expressed in developing xylem and hence their higher occurrence in the FOX library and the resulting increase in phenotypic lines affected in the process. Second, fl-cDNAs overexpressed in the phenotypic lines with changed cell wall composition, were found to be orthologs of *Arabidopsis* genes with involvement in cell wall synthesis like IRREGULAR XYLEM 9 (IRX9), MYB103 and MICROTUBULE ASSOCIATED PROTEIN 65-8 (MAP65-8), FASCICLIN-LIKE ARABINOGLACTAN PROTEIN 17 (FLA17) (Table 3.2). Previous studies linked these genes to secondary cell wall formation (York and O'Neill 2008, Ohman et al. 2013, Ko et al. 2012, Wang et al. 2017). Third, the recovered fl-cDNAs correspond to genes with a high native expression in xylem tissues (Fig 3.5). Collectively, these data strongly suggests the FOX system can preferentially increase the discovery of genes linked in a particular trait, as in this case wood formation.

As mentioned earlier, some of the genes found upregulated in the mutants with altered cell wall composition were of already characterized function. However, 15% of the mutant lines revealed genes of either completely unknown function, having a domain of putative function and/or encoding proteins with putative functions, yet to be characterized (Table 3.2). Cell wall synthesis has been intensively studied for decades because of significant commercial importance to agricultural, forestry and more recently bioenergy industries (Nieminen et al. 2012, Lebedys 2014). Uncovering a significant number of genes not previously characterized in an intensively studied process with a small population is highly encouraging.

## 4.4 Affected Traits Highly Specific to RNA Sampling

Since developing xylem (the tissue used for generation of FOX library) is the main driver of stem girth expansion, we expected an enrichment for lines affected in diameter growth. Unexpectedly, we found an underrepresentation of lines affected in dimeter growth (Fig 3.2). The reasons for this outcome could be multiple. First, the sampling time of the tissue, both in diurnal and seasonal context could have affected the mRNA abundance of specific genes involved in xylem expansion and thus diameter growth (Guerriero, Sergeant, and Hausman 2014). Second, the CZ on the xylem side is only 4-5 cell layers and thus likely disproportionately small percentage of the overall population of sampled cells (Du and Groover 2010). This may have led to low abundance of genes involved in expansion and over-representation of genes involved in cell wall synthesis. Third, genes regulating cambium are typically strong developmental and hormonal regulators: these genes are expressed at very low levels and in a highly cell/tissue specific manner (Du and Groover 2010, Shi et al. 2017). This would have compounded the dilution effect associated with the relative small proportion of sampled CZ cells. Fourth could be simply due to an inadequately short growth time: one study observed a 5-fold increase in the number of phenotypic activation tagged poplars after increasing the growth period (Busov et al. 2011). In summary, we believe the underrepresentation of lines affected in diameter growth is linked to the under-representation of mRNAs representing genes associated with diameter expansion through control of cambium activity. This finding underscores the need for precise sampling tissues for source material for the generation of the FOX library in regards to timing and cell types. Nevertheless, we identified some FOX plants with altered diameter

traits: one of these plants, the 3F16-6 line investigated further because of the significance of the phenotypic changes (discussed in more detail below).

## 4.5 Discovery of *PtaLOG1*'s Role in Xylem Proliferation

As mentioned earlier, 3FOX16.6 showed highly significant phenotypic changes (Fig. 3.6, 3.7, and 3.8). Of particular interest was the increased diameter (Fig. 3.6, and 3.9), suggesting that the gene positively affects secondary growth. Cloning of the inserted fl-cDNA, demonstrating its upregulation, validating increased bioactive cytokinins and most importantly recapitulation of the phenotype in multiple transgenic lines via retransformation of the gene under the same promoter, suggest that upregulation of *PtaLOG1* and increase in bioactive cytokinins are causal for the observed phenotype (Fig. 3.11, 3.12, 3.13, and 3.14).

Although the role of cytokinins in regulation of secondary growth has been known for a while (Ursache, Nieminen, and Helariutta 2013, Immanen et al. 2013), experimental evidence has been largely derived from transgenic manipulations involving heterologous genes, like the *Arabidopsis* Adenosine Phosphate-Isopentenyltransferase 7 (*AtIPT7*) (Immanen et al. 2016) and CYTOKININ OXIDASE 2 (*AtCKX2*) (Nieminen et al. 2008), which led to increased and decreased cytokinin levels respectively. These studies have provided the first and significant insights into the role of cytokinins in regulation of secondary growth in poplars (Nieminen et al. 2008). However, mechanisms detailing bio-molecule regulation of cytokinin levels and signaling are still unclear.

In plants, cytokinin activation uses both the two-step and one-step pathways. The two-step pathway converts cytokinin riboside 5'-monophosphates nucleosides and nucleobases through the activity of nucleotidase and nucleosidase (Dello Loio, Linhares, and Sabatini 2008). In contrast, the direct pathway can produce nucleobases (active cytokinin) from cytokinin riboside 5'-monophosphates through a one-step process (Kuroha et al. 2009) (See Fig 3.11A). The enzyme that catalyzes this step is known as LONELY GUY (LOG), named after the phenotype of the mutant rice plant, which was used to identify the gene, and characterized with severe suppression of stamen development (Kurakawa et al. 2007). LOG is a cytokinin riboside 5'-monophosphate phosphoribohydrolase, and performs the two hydrolase activities leading to cytokinin activation.

Separation of cytokinin biosynthesis from its activation allows for very precise temporal and spatial control of bioactive cytokinins. *PtaLOG1* has the highest expression in xylem tissues and thus may provide a tissue-specific control of bioactive cytokinin levels. *PtaLOG1* shows highest sequence homology to *AtLOG1/3/4* (Fig. 3.10). These three *Arabidopsis* LOGs show distinct substrate specificities from the other LOGs and have identical pH optimum (Kuroha et al. 2009). In the *Arabidopsis* root, *AtLOG3*/4 are targets of LONESOME HIGHWAY (LHW), TARGET OF MONOPTEROS5 (TMO5), as well as its homolog, TMO5-LIKE1(T5L1) (Ohashi-Ito et al. 2014, De Rybel et al. 2013). LHW, TMO5 and T5L1 encode bHLH proteins that form heterodimers to regulate vascular tissue organization (Ohashi-Ito et al. 2014, De Rybel et al. 2013). Moreover, the LHW-T5L1 complex transcriptional activation of LOG3/4 promotes xylem cell fate specification and proliferation (De Rybel et al. 2014). Our data suggests that a similar mechanism may

operate in xylem differentiation and proliferation during secondary woody growth. First, *PtaLOG1* that we have discovered has highest native expression in developing xylem (Fig 3.12). Second, overexpression of *PtaLOG1* resulted in increased secondary growth, specifically through nearly doubling (1.8-fold) xylem proliferation (Fig 3.8). Third, *PtaLOG1* shows very high homology to *AtLOG3/4*, genes implicated in xylem cell specification in the *Arabidopsis* root (De Rybel et al. 2014). Finally, the promoter of *PtaLOG1* contains multiple E-box cis-elements, which have been found to be the binding sites for vascular bHLH regulators like LHW, TMO5 and T5L1 (De Rybel et al. 2014, Liu et al. 2015).

The study conducted by Sundell et al. (2017) had similar interest in this mechanism. Examining *Populus tremula* native expression for *PtLHW* and *PtTMO5* homologs revealed high expression for both genes within xylem expansion region of the stem. Additionally, gene expression of homolog *PtLOG6*, a gene within the same phylogenetic clade as *PtaLOG1* (Fig 3.10), was also incredibly high in the xylem expansion region. Although further investigation needed, these results collectively suggest *PtaLOG1* and other family members of the same clade are key for regulating xylem proliferation.

## 4.6 LOG Biotechnological Applications

Biotechnological manipulation of girth growth is of significant interest because of potential for increasing woody biomass. Here we show that a native poplar LOG gene can significantly increase girth growth. However, because of the ubiquitous expression, transgenic plants also displayed, depending on level of overexpression, reduction in height

growth. This negative effect could likely be overcome using a xylem specific promoter. A recent discovery supports this hypothesis: using an *Arabidopsis* IPT7 gene regulated with a birch xylem specific promoter increased diameter growth in poplar transgenic trees without any negative pleiotropic effects (Immanen et al. 2016). Additionally, because *PtaLOG1* shows homology to multiple *P.trichocarpa* homologs (Fig 3.10), and *PtLOG6* native expression has specificity to xylem expansion (Sundell et al. 2017), it will be important to investigate each genes possible contribution to xylem proliferation using both OE and knock-down lines.

# 5 Conclusions

In regards to our first hypothesis, we concluded the FOX system does generate poplar transformant populations with high mutation rates. Further analysis of the mutant FOX lines confirmed the phenotypes were due to GF: we observed both increases in gene expression specific to fl-cDNAs and the recapitulation of 3FOX16-6 line with multiple *PtaLOG1* OE lines.

Regarding our second hypothesis, we concluded the FOX system could be used for identification of genes specific to xylem development. Using a fl-cDNA library specific to succulent xylem gene expression, we observed (1) a significant enrichment in lines affected with altered cell wall content (lignin, cellulose, and/or hemicellulose); (2) a xylem specific gene expression of *P.trichocarpa* homologs specific to sequenced fl-cDNAs; and (3) multiple mutant FOX lines with fl-cDNA of genes with known function in cell wall development. Additionally, a large proportion of the mutant FOX lines affected in cell wall characteristic trait had fl-cDNAs homologous to genes of unknown function; this demonstrated the FOX system can assist in functional gene discovery with well-studied traits (i.e. cell wall formation).

These results have implications for the FOX systems use as a tool for functional plant genomic studies. We conclude a targeted RNA extraction will enrich a FOX plant population for traits of interest. We reached this conclusion after observing (1) *P.trichocarpa* homologs to our fl-cDNA library with highest native expression in xylem tissue and (2) a great number of mutants affected in traits linked to xylem tissue development. We conclude the FOX system could quicken rates for discovery for

economically and environmentally valuable traits of plant species susceptible to *Agrobacterium* transformation.

Using the FOX system, we observed upregulation of xylem specific *PtaLOG1* greatly increased the development of xylem tissue. Cross-referencing our data with the results of multiple studies, we became interested in multiple LOG gene family members with similar homology to *PtaLOG1* with multiple gene showing roles in xylem proliferation and expansion. We believe the Phylogenetic clade specific to *PtaLOG1* might cluster genes important for regulating xylem girth and therefore should be genetically and biochemically instigated further.

# 6 Reference List


Bhalerao, R. P., and U. Fischer. 2017. "Environmental and hormonal control of cambial stem cell dynamics." *Journal of Experimental Botany* 68 (1):79-87. doi: 10.1093/jxb/erw466.

Brunner, A. M., V. B. Busov, and S. H. Strauss. 2004. "Poplar genome sequence: functional genomics in an ecologically dominant plant species." *Trends Plant Sci* 9 (1):49-56. doi: 10.1016/j.tplants.2003.11.006.

Busov, V. B., A. M. Brunner, R. Meilan, S. Filichkin, L. Ganio, S. Gandhi, and S. H. Strauss. 2005. "Genetic transformation: a powerful tool for dissection of adaptive traits in trees." *New Phytologist* 167 (1):9-18.

Busov, V. B., R. Meilan, D. W. Pearce, C. Ma, S. B. Rood, and S. H. Strauss. 2003a. "Activation tagging of a dominant gibberellin catabolism gene ( GA 2-oxidase ) from poplar that regulates tree stature. ." *Plant Physiol.* 132:1283-1291.

Busov, V. B., R. Meilan, D. W. Pearce, C. Ma, S. B. Rood, and S. H. Strauss. 2003b. "Activation tagging of a dominant gibberellin catabolism gene (GA 2-oxidase) from poplar that regulates tree stature." *Plant Physiol* 132 (3):1283-91.

Busov, V., Y. Yordanov, J. Q. Gou, R. Meilan, C. Ma, S. Regan, and S. Strauss. 2011. "Activation tagging is an effective gene tagging system in Populus." *Tree Genetics & Genomes* 7 (1):91-101.

Carlson, Roger A. 1973. *Statistics*. Edited by Erich L. Lehmann, *Holden-Day Series in Probablilty and Statistics*. San Francisco: Holden-Day, Inc.

Carninci, P., C. Kvam, A. Kitamura, T. Ohsumi, Y. Okazaki, M. Itoh, M. Kamiya, K. Shibata, N. Sasaki, M. Izawa, M. Muramatsu, Y. Hayashizaki, and C. Schneider. 1996. "High-efficiency full-length cDNA cloning by biotinylated CAP trapper." *Genomics* 37 (3):327-336. doi: 10.1006/geno.1996.0567.

Dash, M., Y. S. Yordanov, T. Georgieva, T. J. Tschaplinski, E. Yordanova, and V. Busov. 2017. "Poplar PtabZIP1-like enhances lateral root formation and biomass growth under drought stress." *Plant Journal* 89 (4):692-705. doi: 10.1111/tpj.13413.

De Rybel, B., M. Adibi, A. S. Breda, J. R. Wendrich, M. E. Smit, O. Novak, N. Yamaguchi, S. Yoshida, G. Van Isterdael, J. Palovaara, B. Nijsse, M. V. Boekschoten, G. Hooiveld, T. Beeckman, D. Wagner, K. Ljung, C. Fleck, and D. Weijers. 2014. "Plant development. Integration of growth and patterning during vascular tissue formation in Arabidopsis." *Science* 345 (6197):1255215. doi: 10.1126/science.1255215.

De Rybel, B., B. Moller, S. Yoshida, I. Grabowicz, P. B. de Reuille, S. Boeren, R. S. Smith, J. W. Borst, and D. Weijers. 2013. "A bHLH Complex Controls Embryonic Vascular Tissue Establishment and Indeterminate Growth in Arabidopsis." *Developmental Cell* 24 (4):426-437. doi: 10.1016/j.devcel.2012.12.013.

Dello Loio, R., F. S. Linhares, and S. Sabatini. 2008. "Emerging role of cytokinin as a regulator of cellular differentiation." *Current Opinion in Plant Biology* 11 (1):23-27. doi: 10.1016/j.pbi.2007.10.006.

Dickmann, D. I., Isebrands, J.G., Eckenwalder, J.E., Richardson, J. 2001. *Poplar culture in North America*.

Du, J., and A. Groover. 2010. "Transcriptional Regulation of Secondary Growth and Wood Formation." *Journal of Integrative Plant Biology* 52 (1):17-27.

Dubouzet, J. G., S. Maeda, S. Sugano, M. Ohtake, N. Hayashi, T. Ichikawa, Y. Kondou, H. Kuroda, Y. Horii, M. Matsui, K. Oda, H. Hirochika, H. Takatsuji, and M. Mori. 2011. "Screening for resistance against Pseudomonas syringae in rice-FOX Arabidopsis lines identified a putative receptor-like cytoplasmic kinase gene that confers resistance to major bacterial and fungal pathogens in Arabidopsis and rice." *Plant Biotechnol J* 9 (4):466-85. doi: 10.1111/j.1467-7652.2010.00568.x.

Fujita, M., S. Mizukado, Y. Fujita, T. Ichikawa, M. Nakazawa, M. Seki, M. Matsui, K. Yamaguchi-Shinozaki, and K. Shinozaki. 2007. "Identification of stress-tolerance-related transcription-factor genes via mini-scale Full-length cDNA Over-eXpressor (FOX) gene hunting system." *Biochemical and Biophysical Research Communications* 364 (2):250-257. doi: 10.1016/j.bbrc.2007.09.124.

Gelvin, S. B. 2012. "Traversing the cell: Agrobacterium T-DNA's journey to the host genome." *Frontiers in Plant Science* 3:11. doi: 10.3389/fpls.2012.00052.

Guerriero, G., K. Sergeant, and J. F. Hausman. 2014. "Wood biosynthesis and typologies: a molecular rhapsody." *Tree Physiology* 34 (8):839-855. doi: 10.1093/treephys/tpu031.

Han, K. H., R. Meilan, C. Ma, and S. H. Strauss. 2000. "An Agrobacterium tumefaciens transformation protocol effective on a variety of cottonwood hybrids (genus Populus )." *Plant Cell Reports* 19 (3):315-320.

Higuchi-Takeuchi, M., M. Mori, and M. Matsui. 2013. "High-throughput analysis of rice genes by means of the heterologous full-length cDNA overexpressor (FOX)-hunting system." *Int J Dev Biol* 57 (6-8):517-23. doi: 10.1387/ijdb.130176mm.

Himuro, Y., H. Tanaka, M. Hashiguchi, T. Ichikawa, M. Nakazawa, M. Seki, M. Fujita, K. Shinozaki, M. Matsui, R. Akashi, and F. Hoffmann. 2011. "FOX-superroots of Lotus corniculatus, overexpressing Arabidopsis full-length cDNA, show stable variations in morphological traits." *Journal of Plant Physiology* 168 (2):181-187. doi: 10.1016/j.jplph.2010.10.003.

Ichikawa, T., M. Nakazawa, M. Kawashima, H. Iizumi, H. Kuroda, Y. Kondou, Y. Tsuhara, K. Suzuki, A. Ishikawa, M. Seki, M. Fujita, R. Motohashi, N. Nagata, T. Takagi, K. Shinozaki, and M. Matsui. 2006. "The FOX hunting system: an alternative gain-of-function gene hunting technique." *The Plant Journal* 48 (6):974-985.

Immanen, J., K. Nieminen, O. P. Smolander, M. Kojima, J. A. Serra, P. Koskinen, J. Zhang, A. Elo, A. P. Mahonen, N. Street, R. P. Bhalerao, L. Paulin, P. Auvinen, H. Sakakibara, and Y. Helariutta. 2016. "Cytokinin and Auxin Display Distinct but Interconnected Distribution and Signaling Profiles to Stimulate Cambial Activity." *Current Biology* 26 (15):1990-1997. doi: 10.1016/j.cub.2016.05.053.

Immanen, Juha, Kaisa Nieminen, Héctor Duchens Silva, Fernanda Rodríguez Rojas, Lee A. Meisel, Herman Silva, Victor A. Albert, Torgeir R. Hvidsten, and Ykä Helariutta. 2013. "Characterization of cytokinin signaling and homeostasis gene families in two hardwood tree species: Populus trichocarpa and Prunus persica." *BMC Genomics* 14 (1):885. doi: 10.1186/1471-2164-14-885.

Kaul, S., H. L. Koo, J. Jenkins, M. Rizzo, T. Rooney, L. J. Tallon, T. Feldblyum, W. Nierman, M. I. Benito, X. Y. Lin, C. D. Town, J. C. Venter, C. M. Fraser, S. Tabata, Y. Nakamura, T. Kaneko, S. Sato, E. Asamizu, T. Kato, H. Kotani, S. Sasamoto, J. R. Ecker, A. Theologis, N. A. Federspiel, C. J. Palm, B. I. Osborne, P. Shinn, A. B. Conway, V. S. Vysotskaia, K. Dewar, L. Conn, C. A. Lenz, C. J. Kim, N. F. Hansen, S. X. Liu, E. Buehler, H. Altafi, H. Sakano, P. Dunn, B. Lam, P. K. Pham, Q. Chao, M. Nguyen, G. X. Yu, H. M. Chen, A. Southwick, J. M. Lee, M. Miranda, M. J. Toriumi, R. W. Davis, R. Wambutt, G. Murphy, A. Dusterhoft, W. Stiekema, T. Pohl, K. D. Entian, N. Terryn, G. Volckaert, M. Salanoubat, N. Choisne, M. Rieger, W. Ansorge, M. Unseld, B. Fartmann, G. Valle, F. Artiguenave, J. Weissenbach, F. Quetier, R. K. Wilson, M. de la Bastide, M. Sekhon, E. Huang, L. Spiegel, L. Gnoj, K. Pepin, J. Murray, D. Johnson, K. Habermann, N. Dedhia, L. Parnell, R. Preston, L. Hillier, E. Chen, M. Marra, R. Martienssen, W. R. McCombie, K. Mayer, O. White, M. Bevan, K. Lemcke, T. H. Creasy, C. Bielke, B. Haas, D. Haase, R. Maiti, S. Rudd, J. Peterson, H. Schoof, D. Frishman, B. Morgenstern, P. Zaccaria, M. Ermolaeva, M. Pertea, J. Quackenbush, N. Volfovsky, D. Y. Wu, T. M. Lowe, S. L. Salzberg, H. W. Mewes, S. Rounsley, D. Bush, S. Subramaniam, I. Levin, S. Norris, R. Schmidt, A. Acarkan, I. Bancroft, F. Quetier, A. Brennicke, J. A. Eisen, T. Bureau, B. A. Legault, Q. H. Le, N. Agrawal, Z. Yu, R. Martienssen, G. P. Copenhaver, S. Luo, C. S. Pikaard, D. Preuss, I. T. Paulsen, M. Sussman, A. B. Britt, D. A. Selinger, R. Pandey, D. W. Mount, V. L. Chandler, R. A. Jorgensen, C. Pikaard, G. Juergens, E. M. Meyerowitz, A. Theologis, J. Dangl, J. D. G. Jones, M. Chen, J. Chory, M. C. Somerville, and Ar Gen In. 2000. "Analysis of the genome sequence of the flowering plant Arabidopsis thaliana." *Nature* 408 (6814):796-815.

Ko, J. H., K. H. Han, S. Park, and J. M. Yang. 2004. "Plant body weight-induced secondary growth in Arabidopsis and its transcription phenotype revealed by whole-transcriptome profiling." *Plant Physiology* 135 (2):1069-1083. doi: 10.1104/pp.104.038844.

Ko, J. H., H. T. Kim, I. Hwang, and K. H. Han. 2012. "Tissue-type-specific transcriptome analysis identifies developing xylem-specific promoters in poplar." *Plant Biotechnol J* 10 (5):587-96. doi: 10.1111/j.1467-7652.2012.00690.x.

Kondou, Y., M. Higuchi, and M. Matsui. 2010. "High-Throughput Characterization of Plant Gene Functions by Using Gain-of-Function Technology." In *Annual Review of Plant Biology, Vol 61*, edited by S. Merchant, W. R. Briggs and D. Ort, 373-393. Palo Alto: Annual Reviews.

Kondou, Y., M. Higuchi, S. Takahashi, T. Sakurai, T. Ichikawa, H. Kuroda, T. Yoshizumi, Y. Tsumoto, Y. Horii, M. Kawashima, Y. Hasegawa, T. Kuriyama, K. Matsui, M. Kusano, D. Albinsky, H. Takahashi, Y. Nakamura, M. Suzuki, H. Sakakibara, M. Kojima, K. Akiyama, A. Kurotani, M. Seki, M. Fujita, A. Enju, N. Yokotani, T. Saitou, K. Ashidate, N. Fujimoto, Y. Ishikawa, Y. Mori, R. Nanba, K. Takata, K. Uno, S. Sugano, J. Natsuki, J. G. Dubouzet, S. Maeda, M. Ohtake, M. Mori, K. Oda, H. Takatsuji, H. Hirochika, and M. Matsui. 2009. "Systematic approaches to using the FOX hunting system to identify useful rice genes." *Plant Journal* 57 (5):883-894. doi: 10.1111/j.1365-313X.2008.03733.x.

Kumar, S., G. Stecher, and K. Tamura. 2016. "MEGA7: Molecular Evolutionary Genetics Analysis Version 7.0 for Bigger Datasets." *Molecular Biology and Evolution* 33 (7):1870-1874. doi: 10.1093/molbev/msw054.

Kurakawa, T., N. Ueda, M. Maekawa, K. Kobayashi, M. Kojima, Y. Nagato, H. Sakakibara, and J. Kyozuka. 2007. "Direct control of shoot meristem activity by a cytokinin-activating enzyme." *Nature* 445 (7128):652-655. doi: 10.1038/nature05504.

Kuroha, T., H. Tokunaga, M. Kojima, N. Ueda, T. Ishida, S. Nagawa, H. Fukuda, K. Sugimoto, and H. Sakakibara. 2009. "Functional analyses of LONELY GUY cytokinin-activating enzymes reveal the importance of the direct activation pathway in Arabidopsis." *Plant Cell* 21. doi: 10.1105/tpc.109.068676.

Lebedys, A., and Y. Li. 2014. Contribution of the Forestry Sector to National Economies, 1990-2011. edited by Policy and Products Division Forestry Department Forest Economics. Rome: Food and Agriculture Organization of the United Nations.

Levyadun, S. 1994. "Induction of Sclereid differentiation in the pith of Arabidopsis thaliana (L.) Heynh." *Journal of Experimental Botany* 45 (281):1845-1849. doi: 10.1093/jxb/45.12.1845.

Li, L. G., S. F. Lu, and V. Chiang. 2006. "A genomic and molecular view of wood formation." *Critical Reviews in Plant Sciences* 25 (3):215-233. doi: 10.1080/07352680600611519.

Lin, Y. C., W. Li, H. Chen, Q. Li, Y. H. Sun, R. Shi, C. Y. Lin, J. P. Wang, H. C. Chen, L. Chuang, G. Z. Qu, R. R. Sederoff, and V. L. Chiang. 2014. "A simple improved-throughput xylem protoplast system for studying wood formation." *Nature Protocols* 9 (9):2194-2205. doi: 10.1038/nprot.2014.147.

Liu, L. J., V. Filkov, and A. Groover. 2014. "Modeling transcriptional networks regulating secondary growth and wood formation in forest trees." *Physiologia Plantarum* 151 (2):156-163. doi: 10.1111/ppl.12113.

Liu, Yujia, Xiaoyu Ji, Xianguang Nie, Min Qu, Lei Zheng, Zilong Tan, Huimin Zhao, Lin Huo, Shengnan Liu, Bing Zhang, and Yucheng Wang. 2015. "Arabidopsis AtbHLH112 regulates the expression of genes involved in abiotic stress tolerance by binding to their E-box and GCG-box motifs." *New Phytologist* 207 (3):692-709. doi: 10.1111/nph.13387.

Nakamura, H., M. Hakata, K. Amano, A. Miyao, N. Toki, M. Kajikawa, J. Pang, N. Higashi, S. Ando, S. Toki, M. Fujita, A. Enju, M. Seki, M. Nakazawa, T. Ichikawa, K. Shinozaki, M. Matsui, Y. Nagamura, H. Hirochika, and H. Ichikawa. 2007. "A genome-wide gain-of-function analysis of rice genes using the FOX-hunting system." *Plant Molecular Biology* 65 (4):357-371. doi: 10.1007/s11103-007-9243-y.

Nieminen, K., J. Immanen, M. Laxell, L. Kauppinen, P. Tarkowski, K. Dolezal, S. Tahtiharju, A. Elo, M. Decourteix, K. Ljung, R. Bhalerao, K. Keinonen, V. A. Albert, and Y. Helariutta. 2008. "Cytokinin signaling regulates cambial development in poplar." *Proceedings of the National Academy of Sciences of the United States of America* 105 (50):20032-20037.

Nieminen, K., M. Robischon, J. Immanen, and Y. Helariutta. 2012. "Towards optimizing wood development in bioenergy trees." *New Phytologist* 194 (1):46-53. doi: 10.1111/j.1469-8137.2011.04011.x.

Ohashi-Ito, K., M. Saegusa, K. Iwamoto, Y. Oda, H. Katayama, M. Kojima, H. Sakakibara, and H. Fukuda. 2014. "A bHLH Complex Activates Vascular Cell Division via Cytokinin Action in Root Apical Meristem." *Current Biology* 24 (17):2053-2058. doi: 10.1016/j.cub.2014.07.050.

Ohman, D., B. Demedts, M. Kumar, L. Gerber, A. Gorzsas, G. Goeminne, M. Hedenstrom, B. Ellis, W. Boerjan, and B. Sundberg. 2013. "MYB103 is required for FERULATE-5-HYDROXYLASE expression and syringyl lignin biosynthesis in Arabidopsis stems." *Plant Journal* 73 (1):63-76. doi: 10.1111/tpj.12018.

Plett, J. M., O. Wilkins, M. M. Campbell, S. G. Ralph, and S. Regan. 2010. "Endogenous overexpression of Populus MYB186 increases trichome density, improves insect pest resistance, and impacts plant growth." *Plant Journal* 64 (3):419-432. doi: 10.1111/j.1365-313X.2010.04343.x.

Ruzicka, K., R. Ursache, J. Hejatko, and Y. Helariutta. 2015. "Xylem development - from the cradle to the grave." *New Phytologist* 207 (3):519-535. doi: 10.1111/nph.13383.

Sakakibara, H. 2006. "Cytokinins: Activity, biosynthesis, and translocation." *Annual Review of Plant Biology* 57:431-449. doi: 10.1146/annurev.arplant.57.032905.105231.

Seki, M., P. Carninci, Y. Nishiyama, Y. Hayashizaki, and K. Shinozaki. 1998. "High-efficiency cloning of Arabidopsis full-length cDNA by biotinylated CAP trapper." *Plant J* 15 (5):707-20.

Seki, M., M. Narusaka, J. Ishida, T. Nanjo, M. Fujita, Y. Oono, A. Kamiya, M. Nakajima, A. Enju, T. Sakurai, M. Satou, K. Akiyama, T. Taji, K. Yamaguchi-Shinozaki, P. Carninci, J. Kawai, Y. Hayashizaki, and K. Shinozaki. 2002. "Monitoring the expression profiles of 7000 Arabidopsis genes under drought, cold and high-salinity stresses using a full-length cDNA microarray." *Plant J* 31 (3):279-92.

Seki, M., M. Narusaka, A. Kamiya, J. Ishida, M. Satou, T. Sakurai, M. Nakajima, A. Enju, K. Akiyama, Y. Oono, M. Muramatsu, Y. Hayashizaki, J. Kawai, P. Carninci, M. Itoh, Y. Ishii, T. Arakawa, K. Shibata, A. Shinagawa, and K. Shinozaki. 2002. "Functional annotation of a full-length Arabidopsis cDNA collection." *Science* 296 (5565):141-5. doi: 10.1126/science.1071006.

Seki, M., and K. Shinozaki. 2009. "Functional genomics using RIKEN Arabidopsis thaliana full-length cDNAs." *Journal of Plant Research* 122 (4):355-366. doi: 10.1007/s10265-009-0239-3.

Shi, R., J. P. Wang, Y. C. Lin, Q. Z. Li, Y. H. Sun, H. Chen, R. R. Sederoff, and V. L. Chiang. 2017. "Tissue and cell-type co-expression networks of transcription factors and wood component genes in Populus trichocarpa." *Planta* 245 (5):927-938. doi: 10.1007/s00425-016-2640-1.

Sneath, P. H. A., and R. R. Sokal. 1973. *Numerical taxonomy. The principles and practice of numerical classification*. San Francisco, W.H. Freeman and Company.

Sundell, D., N. R. Street, M. Kumar, E. J. Mellerowicz, M. Kucukoglu, C. Johnsson, V. Kumar, C. Mannapperuma, N. Delhomme, O. Nilsson, H. Tuominen, E. Pesquet, U. Fischer, T. Niittyla, B. Sundberg, and T. R. Hvidsten. 2017. "AspWood: High-Spatial-Resolution Transcriptome Profiles Reveal Uncharacterized Modularity of Wood Formation in Populus tremula." *Plant Cell* 29 (7):1585-+. doi: 10.1105/tpc.17.00153.

Thomas, Richard H. 2001. "Molecular Evolution and Phylogenetics." *Heredity* 86 (3):385-385.

Tokunaga, H., M. Kojima, T. Kuroha, T. Ishida, K. Sugimoto, T. Kiba, and H. Sakakibara. 2012. "Arabidopsis lonely guy (LOG) multiple mutants reveal a central role of the LOG-dependent pathway in cytokinin activation." *Plant J* 69. doi: 10.1111/j.1365-313X.2011.04795.x.

Tuskan, G. A., S. Difazio, S. Jansson, J. Bohlmann, I. Grigoriev, U. Hellsten, N. Putnam, S. Ralph, S. Rombauts, A. Salamov, J. Schein, L. Sterck, A. Aerts, R. R. Bhalerao, R. P. Bhalerao, D. Blaudez, W. Boerjan, A. Brun, A. Brunner, V. Busov, M. Campbell, J. Carlson, M. Chalot, J. Chapman, G. L. Chen, D. Cooper, P. M. Coutinho, J. Couturier, S. Covert, Q. Cronk, R. Cunningham, J. Davis, S. Degroeve, A. Dejardin, C. Depamphilis, J. Detter, B. Dirks, I. Dubchak, S. Duplessis, J. Ehlting, B. Ellis, K. Gendler, D. Goodstein, M. Gribskov, J. Grimwood, A. Groover, L. Gunter, B. Hamberger, B. Heinze, Y. Helariutta, B. Henrissat, D. Holligan, R. Holt, W. Huang, N. Islam-Faridi, S. Jones, M. Jones-Rhoades, R. Jorgensen, C. Joshi, J. Kangasjarvi, J. Karlsson, C. Kelleher, R. Kirkpatrick, M. Kirst, A. Kohler, U. Kalluri, F. Larimer, J. Leebens-Mack, J. C. Leple, P. Locascio, Y. Lou, S. Lucas, F. Martin, B. Montanini, C. Napoli, D. R. Nelson, C. Nelson, K. Nieminen, O. Nilsson, V. Pereda, G. Peter, R. Philippe, G. Pilate, A. Poliakov, J. Razumovskaya, P. Richardson, C. Rinaldi, K. Ritland, P. Rouze, D. Ryaboy, J. Schmutz, J. Schrader, B. Segerman, H. Shin, A. Siddiqui, F. Sterky, A. Terry, C. J. Tsai, E. Uberbacher, P. Unneberg, J. Vahala, K. Wall, S. Wessler, G. Yang, T. Yin, C. Douglas, M. Marra, G. Sandberg, Peer Y. Van de, and D. Rokhsar. 2006. "The genome of black cottonwood, Populus trichocarpa (Torr. & Gray)." *Science.* 313 (5793):1596-1604.

Ursache, Robertas, Kaisa Nieminen, and Ykä Helariutta. 2013. "Genetic and hormonal regulation of cambial development." *Physiologia Plantarum* 147 (1):36-45. doi: 10.1111/j.1399-3054.2012.01627.x.

Wang, Haihai, Yanli Jin, Cuiting Wang, Bei Li, Chunmei Jiang, Zhencang Sun, Zhiping Zhang, Fanjing Kong, and Hongxia Zhang. 2017. "Fasciclin-like arabinogalactan proteins, PtFLAs, play important roles in GA-mediated tension wood formation in Populus." *Scientific Reports* 7 (1):6182. doi: 10.1038/s41598-017-06473-9.

Wasteneys, G. O. 2002. "Microtubule organization in the green kingdom: chaos or self-order?" *Journal of Cell Science* 115 (7):1345-1354.

Weigel, D., J. H. Ahn, M. A. Bl…zquez, J. O. Borevitz, S. K. Christensen, C. Fankhauser, C. Ferr…ndiz, I. Kardailsky, E. J. Malancharuvil, M. M. Neff, J. T. Nguyen, S. Sato, Z. Y. Wang, Y. Xia, R. A. Dixon, M. J. Harrison, C. J. Lamb, M. F. Yanofsky, and J. Chory. 2000. "Activation tagging in Arabidopsis." *Plant Physiol.* 122 (4):1003-1013.

Weigel, D., Glazebrook, J. 2002. *Arabidopsis: A Laboratory Manual*. Cold Spring Harbor, NY: Cold Spring Harbor Laboratory Press.

Yordanov, Y. S., C. Ma, S. H. Strauss, and V. B. Busov. 2014. "EARLY BUD-BREAK 1 (EBB1) is a regulator of release from seasonal dormancy in poplar trees." *Proceedings of the National Academy of Sciences of the United States of America* 111 (27):10001-10006. doi: 10.1073/pnas.1405621111.

York, W. S., and M. A. O'Neill. 2008. "Biochemical control of xylan biosynthesis - which end is up?" *Curr Opin Plant Biol* 11 (3):258-65. doi: 10.1016/j.pbi.2008.02.007.

Zhang, J., K. Nieminen, J. A. A. Serra, and Y. Helariutta. 2014. "The formation of wood and its control." *Current Opinion in Plant Biology* 17:56-63. doi: 10.1016/j.pbi.2013.11.003.

Zhang, Jianxing, Evandro Novaes, Matias Kirst, and Gary Peter. 2014. "Comparison of Pyrolysis Mass Spectrometry and Near Infrared Spectroscopy for Genetic Analysis of Lignocellulose Chemical Composition in Populus." *Forests* 5 (3):466.

# A Plasmids Used

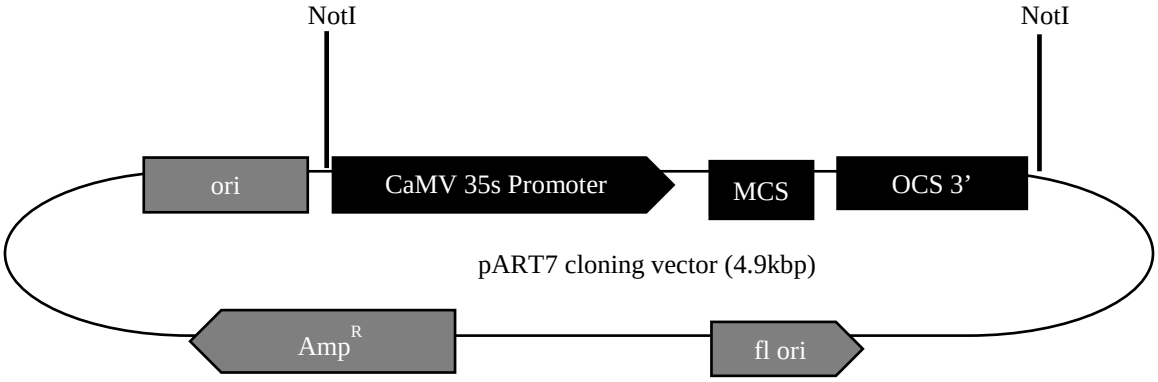


**Figure A.1:** pART7 plant cloning vector.

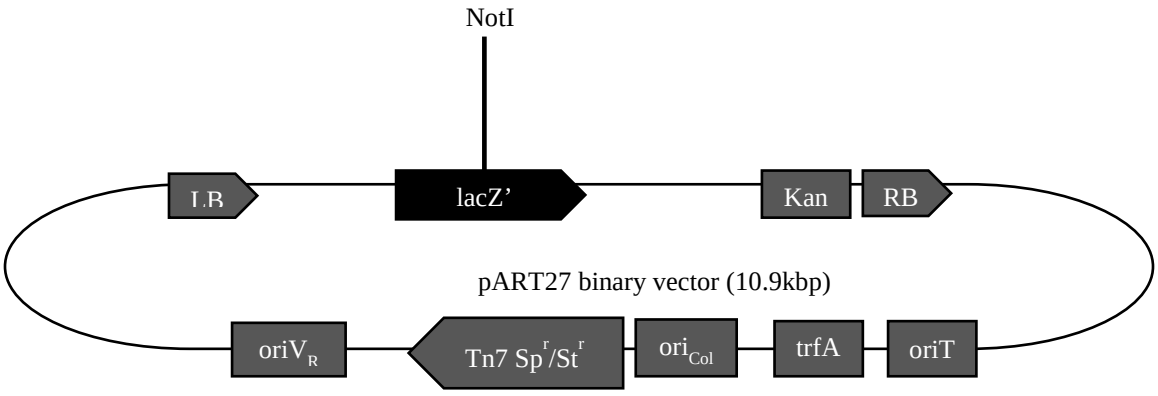


**Figure A.2:** pART27 plant binary vector.

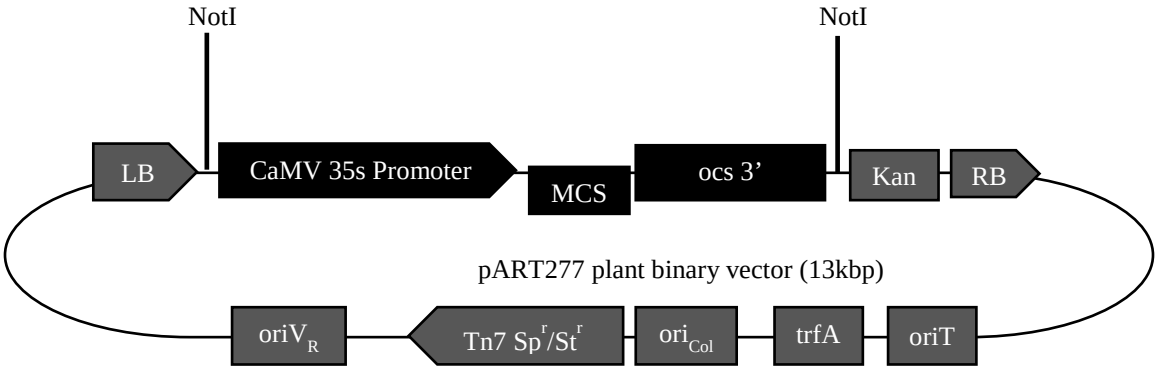


**Figure A.3:** pART277 plant binary vector. Used as the FOX vector. This vector was engineered using the region of the pART7 vector spanning from the CaMV 35S promoter to the OCS terminator (Fig. A.1) and the pART27 vector backbone (Fig. A.2): this was completed using a NotI restriction digestion (D.1), isolation and purification of correctly digested fragments (C.2), and T4 ligation (D.2). The multi cloning site (MCS) site of pART277 was further modified to accommodate the generation of the FOX library. Bio S&T Inc. (Quebec, Canada) performed all modifications. Specifically, two existing SfiI sites were removed from existing MCS and SfiIAB sites (5´-GGC CAT TAC GGC CAA CCT TGA TAT CGG CCG CCT CGG CC-3´) were inserted into the MCS (between EcoRI and HindIII).

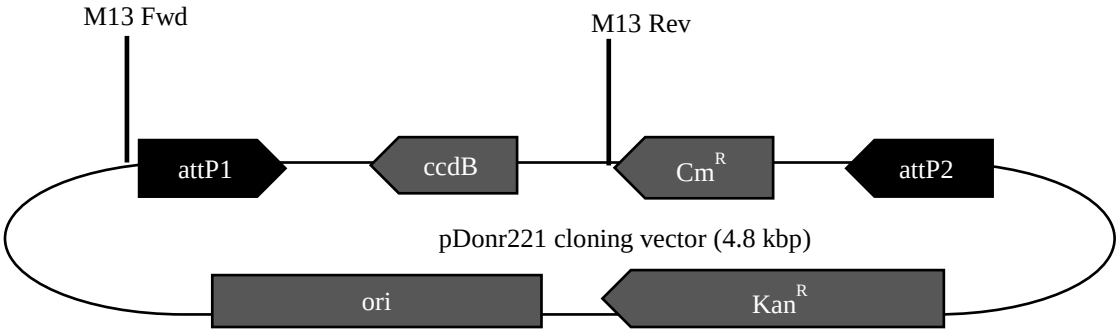


**Figure A.4:** pDonr221 cloning vector.

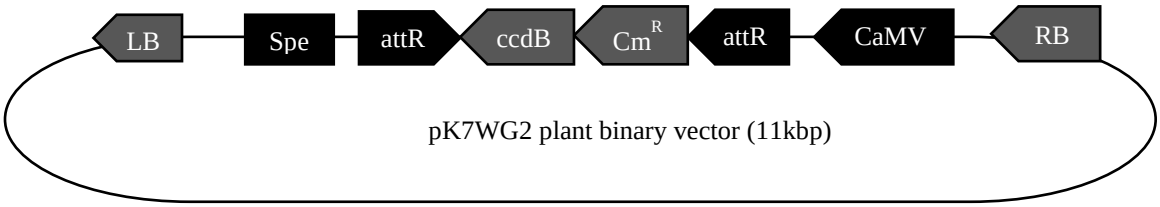


**Figure A.5:** pK7WG2 plant binary vector.

# B Primer Detail

## B.1 Primers List

**Table B.1:** All primers used for experimentation. Designed using NCBI PrimerBLAST tool.

| Primer Name | Sequence (5'→3') | Annealing Temperature | Primer purpose |
|---|---|---|---|
| **Oligo(dT)$_{18}$** | TTTTTTTTTTTTTTTTT | | Reverse transcription |
| **Random oligonucleotides(dN)$_{18}$** | NNNNNNNNNNNNNNNNN | 58°C | Reverse transcription |
| **Pro35s F** | CCACTGACGTAAGGGATGACGCACA | 66.3 | Cloning |
| **ocsCZ R** | ATTAGTTCGCCGCTCGGTG | 57.9 | Cloning |
| **Npt II F** | ATCAGGATGATCTGGACGAAGAG | 62.8 | Transformation validation |
| **Npt II R** | GATACCGTAAAGCACGAGGAAG | 62.7 | Transformation validation |
| **B1 Pro35s F** | GGGGACAAGTTTGTACAAAAAAGCAGGCTGGCCACTGACGTAAGGGATGACGCACA | 66.3 | Cloning |
| **B2 ocsCZ R** | GGGGACCACTTTGTACAAGAAAGCTGGGTCATTAGTTCGCCGCTCGGTG | 57.9 | Cloning |
| **Ubiq F** | AAGAGTGTGAGAGAGAGAAGA | 56.0 | qRT-PCR |
| **Ubiq R** | CCACGACCATCAAACAAGAAG | 64.4 | qRT-PCR |
| **1FOX1-3F** | GGTGTGGACTGTGCGTTAGA | 62.4 | qRT-PCR |
| **1FOX1-3R** | TGGAAAAGTGCCGGTGAGAA | 60.4 | qRT-PCR |
| **1FOX3-4F** | GACTTGGATGCTTGATCCATCAGA | 62.9 | qRT-PCR |
| **1FOX3-4R** | GCATCCGAAGCAGCAGTGGA | 64.5 | qRT-PCR |
| **1FOX3-9F** | CAGGTTGGTTCCTCCACCAT | 62.4 | qRT-PCR |
| **1FOX3-9R** | ACGATTCCCACTCAGCTTGT | 60.4 | qRT-PCR |
| **1FOX43-3F** | GCATAACGGAGTATGGAGACTC | 62.7 | qRT-PCR |
| **1FOX43-3R** | TGACTGCACGGTCCTACTCA | 62.4 | qRT-PCR |
| **1FOX46-1F** | TGGTGGAGGTTTCGAGTTTC | 60.4 | qRT-PCR |
| **1FOX46-1R** | CCCACATTGCCTTTGTTTCT | 58.4 | qRT-PCR |

| Primer Name | Sequence (5'→3') | Annealing Temperature | Primer purpose |
|---|---|---|---|
| **2FOX1-1R** | TTGGTCCTTGCTCTTCGGTT | 60.4 | qRT-PCR |
| **2FOX1-1F** | CCTCTTGCTCTCGTGACAGT | 62.4 | qRT-PCR |
| **2FOX5-2F** | CAGACTGGCTTTGGTTGCTG | 62.4 | qRT-PCR |
| **2FOX5-2R** | TCTTCACCATTGGCTGTCCC | 62.4 | qRT-PCR |
| **3FOX10-5F** | ACGAAGAAGCTGCTGATGGT | 60.4 | qRT-PCR |
| **3FOX10-5R** | ACAGGCATACCAGGAGTTGG | 62.4 | qRT-PCR |
| **3FOX10-7F** | TCCGCCGTAGAATGGACATC | 62.4 | qRT-PCR |
| **3FOX10-7R** | GTGCTCGAAGAAACACGCAA | 60.4 | qRT-PCR |
| **3FOX12-7F** | GGGAGAGGGCATGAACGAAT | 62.4 | qRT-PCR |
| **3FOX12-7R** | CGAGCACCCCTAGTGTGATG | 64.5 | qRT-PCR |
| **3FOX16-5F** | AGCAACGAAAGCGCATCTAT | 58.4 | qRT-PCR |
| **3FOX16-5R** | GCAACCAGAGGTCCAAATGT | 60.4 | qRT-PCR |
| **3FOX16-6F** | GGCCGTCATGTGATTGGAGT | 62.4 | qRT-PCR |
| **3FOX16-6R** | CACATTCAGCAATCCCACCG | 62.4 | qRT-PCR |
| **3FOX903.1F** | TTTTCAGAGAAAGAGAGCCTTTTGGT | 60.1 | qRT-PCR |
| **3FOX90-3.1R** | CTGAACAAAAGCCAACGCCA | 60.4 | qRT-PCR |
| **3FOX90-3.2R** | CCAGGAACTCCATAAACTTCTGTAC | 62.9 | qRT-PCR |
| **3FOX90-3.2F** | GGAATTCTCGTGGACCGTGT | 62.4 | qRT-PCR |

## B.2 Primer Targeting Sites

TCGACGAATTAATTCCAATCCCACAAAAATCTGAGCTTAACAGCACAGTTGCTCCTCTCAGAGCAGAATCG
GGTATTCAACACCCTCATATCAACTACTACGTTGTGTATAACGGTCCACATGCCGGTATATACGATGACTG
GGGTTGTACAAAGGCGGCAACAAACGGCGTTCCCGGAGTTGCACACAAGAAATTTGCCACTATTACAGAGG
CAAGAGCAGCAGCTGACGCGTACACAACAAGTCAGCAAACAGACAGGTTGAACTTCATCCCCAAAGGAGAA
GCTCAACTCAAGCCCAAGAGCTTTGCTAAGGCCCTAACAAGCCCACCAAAGCAAAAAGCCCACTGGCTCAC
GCTAGGAACCAAAAGGCCCAGCAGTGATCCAGCCCCAAAAGAGATCTCCTTTGCCCCGGAGATTACAATGG
ACGATTTCCTCTATCTTTACGATCTAGGAAGGAAGTTCGAAGGTGAAGGTGACGACACTATGTTCACCACT
GATAATGAGAAGGTTAGCCTCTTCAATTTCAGAAAGAATGCTGACCCACAGATGGTTAGAGAGGCCTACGC
AGCAGGTCTCATCAAGACGATCTACCCGAGTAACAATCTCCAGGAGATCAAATACCTTCCCAAGAAGGTTA
AAGATGCAGTCAAAAGATTCAGGACTAATTGCATCAAGAACACAGAGAAAGACATATTTCTCAAGATCAGA
AGTACTATTCCAGTATGGACGATTCAAGGCTTGCTTCATAAACCAAGGCAAGTAATAGAGATTGGAGTCTC
TAAAAAGGTAGTTCCTACTGAATCTAAGGCCATGCATGGAGTCTAAGATTCAAATCGAGGATCTAACAGAA
CTCGCCGTGAAGACTGGCGAACAGTTCATACAGAGTCTTTTACGACTCAATGACAAGAAGAAAATCTTCGT
CAACATGGTGGAGCACGACACTCTGGTCTACTCCAAAAATGTCAAAGATACAGTCTCAGAAGACCAAAGGG
CTATTGAGACTTTTCAACAAAGGATAATTTCGGGAAACCTCCTCGGATTCCATTGCCCAGCTATCTGTCAC
TTCATCGAAAGGACAGTAGAAAAGGAAGGTGGCTCCTACAAATGCCATCATTGCGATAAAGGAAAGGCTAT
CATTCAAGATCTCTCTGCCGACAGTGGTCCCAAAGATGGACCCCCACCCACGAGGAGCATCGTGGAAAAAG
AAGACGTTCCAACCACGTCTTCAAAGCAAGTGGATTGATGTGACATCTCCACTGACGTAAGGGATGACGCA
CAATCCCACTATCCTTCGCAAGACCCTTCCTCTATATAAGGAAGTTCATTTCATTTGGAGAGGACACG

**Figure B2.1:** Anchoring site of Pro35s F within the FOX promoter based on sequence from pART277 plant binary vector.

CTGCTTTAATGAGATATGCGAGACGCCTATGATCGCATGATATTTGCTTTCAATTCTGTTGTGCACGTTGT
AAAAAACCTGAGCATGTGTAGCTCAGATCCTTACCGCCGGTTTCGGTTCATTCTAATGAATATATCACCCG
TTACTATCGTATTTTTATGAATAATATTCTCCGTTCAATTTACTGATTGTACCCTACTACTTATATGTACA
ATATTAAAATGAAAACAATATATTGTGCTGAATAGGTTTATAGCGACATCTATGATAGAGCGCCACAATAA
CAAACAATTGCGTTTTATTATTACAAATCCAATTTTAAAAAAAGCGGCAGAACCGGTCAAACCTAAAAGAC
TGATTACATAAATCTTATTCAAATTTCAAAAGGCCCCAGGGGCTAGTATCTACGACACACCGAGCGGCGAA
CTAATAACGTTCACTGAAGGGAACTCCGGTTCCCCGCCGGCGCGCATGGGTGAGATTCCTTGAAGTTGAGT
ATTGGCCGTCCGCTCTACCGAAAGTTACGGGCACCATTCAACCCGGTCCAGCACGGCGGCCGGGTAACCGA
CTTGCTGCCCCGAGAATTATGCAGCATTTTTTTGGTGTATGTGGGCCCCAAATGAAGTGCAGGTCAAACCT
TGACAGTGACGACAAATCGTTGGGCGGGTCCAGGGCGAATTTTGCGACAACATGTCGAGGCTCAGCAGGAC
CTGCAGGCATGCAAGCTAGCTTACTAGTGATGCATATT

**Figure B2.2:** Anchoring site of ocsCZ R within the FOX terminator based on sequence from pART277 plant binary vector.

GTTCATGGAAGATTGTCCTATCAGATGCTTAAACCCGACCCTGTCCTGAGGAATATCTTACTTAATGTGCC
TGTTCGTAAAGTTGTCTTTACCAATGCTGATAAGGCTCATGCAAGTCGAGTCCTTAGCAGGCTTGGATTGG
AGGATTGTTTTGAAAGGATCATATGCTTTGAGACTTTGAATGATGCTGCTAATAAAGGAAATGATCCTGTT
GATGGGGATGACAGAGAGGTTTTTGACTTCGATGAATATACTACCTGTCCTGATGCAGATCTTGTACCTCC
AAGGACCCCTGTGGTCTGCAAACCCTTTGAGGAAGCATTTGAGCAGGTTTTTAAGATCGCCGGCATCAGCC
CTCAAAAGACGTCGTTCTTTGATGATAGCATCCGTAACATACAGACTGGAAAAGGATTGGGTCTCCACACT
GTTTGGGTAGGCTCTTCTCATCGGATTGAAGGTGTGGACTGTGCGTTAGAGAGTCTTCATAATATCAAGGA
AGCACTGCCAGAACTCTGGGAAGCTAATGATAAGTCTGAAGCCATCAAGTATTCCAAGAAAGTTGCAATTG
AGACATCTGTGGAAGCTTAGCTAATTATTATTTTACTACTATTATTGTATTTCTCACCGGCACTTTTCCA
TTACCATCTCTGTATTTTATATTCAGTGGGGGCTGAACATCTGAatgTTATTACGTTCTAATTATATTATA
GTAATTTAAATAGAGCACTCTGTTAGTGTGATTAAAAAAAAAAAAAAAAGCCGCCTCGCATCGATAGCTTGA
TCTCTAGGAGTCTGCTTAATGGAGAATATGCGGAGACGCCTGGAACCCAGCCAT

**Figure B2.3:** Anchoring sites for qRT-PCR 1FOX1-3 specific primers within the fl-cDNA insert of HALOACID DEHALOGENASE-LIKE HYDROLASE (HAD) gene sequence

GGGGGATCCCGCAGATCTCGAGGTTGAACATATATTTGAAGTGGGTGAGTGGGTGAAACTGAGGGAAGATG
TTAGTAACTGGAAATCTGTTGGACCAGGCAGTGTGGGTGTTGTACAGGGTATAGGATATGATGGAGATGAG
TGGGATGGAAGCATATATGTTGGTTTTTGTGGGGAGCAAGAAAGATGGGCGGGGCCTACTTCCCATCTTGA
AAGAGTTGAAAGACTCATGGTTGGGCAGAAAGTTAGGGTTAAACTTTCTGTGAAGCAGCCAAGGTTTGGGT
GGTCAAGCCACAGTCATGGAAGTGTTGGAACCATATCGGCAATTGATGCTGATGGGAAGCTGAGAATATAT
ACTCCAGTAGGCTCCAAGACTTGGATGCTTGATCCATCAGAAGTGGAGGTGGTAGAGGATGAAGAACTTCA
CATTGGAGATTGGGTGAAAGTAAGGGCATCCGTTTCCCCACCAACACGCCCCCCCTTTATAACTAAAAAAA
ATCAAACACTCCACTGCTGCTTCGGATGCCCCCACGCCCACCGTGTCCGTTTTGTTCTGTTTCCTCTCTTC
CCCACCCCGCCCCGCGGTGTTTCGGACACTGCTCACAAATTTTCACCCTTGCCCCCCTCCGTGGAGAAGGG
GCAAATTCTTTCCATTTCCGAAACCTCCGCAAACCCCAGGCTGTCTACCAGAAAAAAAAAGAAAACACCAA
GTCCCCCCCCTTTTTCTATCCAGGACACCCCCACCCATTGTATGGATGATTCCCTCTCTCCCCCCCCGGGTG
TGTGTGTGGTTTTGTAAAACGCGGACGCCACCAACCCTTCCCCCCCAATCCTCTCCAAGAGTGGAGATTTT
TTTTATTTCTTTTCACGTGTTCATTTCTTGAAGAATAAAAGAGGCAGAATGTCTTTGGAGACCCCATCGCG
GAGAATCTAAT

**Figure B2.4:** Anchoring sites for qRT-PCR 1FOX3-4 specific primers within the fl-cDNA insert of KEEP ON GOING (KEG) gene sequence.

GGTCTTCCACATCTCTCAATCTCTCTCAAAGAATCCCTTTCTTTTTCCCCAAAACTCAGGGGTCAGTATCT
GAGCCAACAACTTGGTTTTTGATCACGTTTTTGAGAGGTTTAGCTTGATGGGCTCTGTGGAAAGATCAAAG
AGGAGAGTTCAGTTATGGAAGAAAGCTATAGTTCATTTTGGTTTGTGTTTTGTTATGGGGTTTTTCACAGG
TTTCGCTCCAGCAGGCAAGGCTTCAATTTTTACTAGTCATGTTGCTGCATCAAATAAATCGCAATCCTTGC
CGCAACCTGTTGAAATGTTGCACCAGCAGGCAGCAAGTGCACCACATGCTAGTAATGTCAACAGAAGTTTG
ATAGCTGAAACTGCAGTACCAGCTCCACCAAGCTCTAAGGAATCTGAACATGCAGCATTCTTGGAAAAAGA
AGAAACAGAATCCAAGTTAGCGCCAAGAAGACTGGCAATCATCGTTACGCCAACAAGCACTAAAGATCCGT
ATCAAGGGGTTTTCTTGAGGAGGTTGGCTAACACGATCAGGTTGGTTCCTCCACCATTATTGTGGATTGTT
GTGGAAAGGCAATCAGATTCAGATGAAATATCGGAGGTCCTTAGGAAAACAGGTATTATGTATAGGCATTT
GGTGTTCAAGGAGAATTTTACAGATCCCGAAGCAGAGTTGGGATCATCAAAGGAATGTAGCATTAATGCAC
ATTGAAAAAACACAAGCTGAGTGGGAATCGTTCATTTCTGCCCGGGCCTTTCCAATGATTACGATCGTGGG
CATTCTTTGACGAGATTAGACAAACTTGACGGTGTTAGGAAACATGGCTCGATGGCAGATACTTAAGACTA
GCTGAGAGAACGTGTCATGCAAGTGACTCTGTTATTGTCATTCCTTGACA

**Figure B2.5:** Anchoring sites for qRT-PCR 1FOX3-9 specific primers within the fl-cDNA insert of IRREGULAR XYLEM 9 (IRX9) gene sequence.

ACGTCACCTTCAACTTCAACACGAAAAGAGGAAGAAAAGACCGTTTCAAACTATCACCGTTTTAAACCATC
ACTGATCGCTCAAAAAATGCTTTCTGCGACGATAGGAATCCTTTAAAACGACAACAAAATCCAGTCATGTC
AACCTCAAGCTCAACCACGGCGACGTCGTTTTTATCAGCGACGCAGAGATACGCAGCCGGAGCATTATTTG
CAATCGCTCTTCACCAAGCACAGATCCATCAAACCCGTCCGCTTGGCTTATCCCACGATGACTCGGAACAA
GAGGAACGAACCAGTTGCAGCAGTAGTCATAGTAATGGCAGCAGCAGTGATTCCGTTTCTGAAGACCCTGA
CCTTTGGATCCACGAAAATTCGGGCCTCCTCCGACCCGTATTCAGGTTTTTAGAGGTTGAGTCAGTAGCAT
GGACTGGACTTGAAGAGACAGCTGGTGGTTCTCCTGCTAAGCATCATGTTGGATCTTTCTTGAGGTTATTA
TCAGAAGAAAGTGGCAATGCGGCTTCTTCTTCTTCTCAAAGTTCGGATCAAGAAGTTGCTTTATCAAAGGC
TGTGATGTAATGGAAGAAACCATGGGGAGCGAATCCTGTGTCGTCCCAGTCTAGGAAGGAGAAGCATAACG
GAGTATGGAGACTCATGCCGTGAAAGTTATCTGCTGCAGTGAGGTGAATCACCTCTGAGGTGGAAAATGAT
CACAAAACTGCAAGGATGAACATCGCTGGAGTTAACGGATGCCACCTTGAACCTTGGACATATGTTGAGTA
GGACCGTGCAGTCAAAGTCTATGTTATCAAGAACTGGACTGGCTGTCGA

**Figure B2.6:** Anchoring sites for qRT-PCR 1FOX43-3 specific primers within the fl-cDNA insert of a DUF726 gene sequence.

GGATATGTTAGGCAGAGCTGGAAGAATTGATGATGCATTGGTGGTGGTGAAAAACATGCCCATGAAGACAA
GTGGTAGCATATGGGGATCATTGCTCAACTCATGCCGCCTACATAACGAGGTCCCTCTTGCCGAGGCTATT
GCAAACCAGTTGTTTGAGCTTGAGCCATGTAATCCTGGGAACTATGTGATGCTCTCAAACATTTATGCAAA
TGCAGGGATGTGGGACTCTGTAAATATGGTTAGAGAGATGATGCAAAAAAGAAGAATCAGAAAAGAGGCTG
GATGTAGTTGGATACAGGTAAAGAATAAAATCCACTCTTTTGTAGCTGGTGGAGGTTTCGAGTTTCGTAAT
TCTGATGAATATAAGAAGATATGGAACAAAGTAAGGGAAGCCATGGAAGAATTTGGTTATATACCCAACAC
AGATGTGGTGCTTCATGATGTAAATGAAGAAACAAAGGCAATGTGGGTGTGTGGGCACAGTGAGCGCTTAG
CAACTGTTTTTTCTCTGATACATACTGCTGCCGGAATGCCAATCAGGATAACAAAGAACCTTCGTGTTTGT
GTAGATTGTCACTCTTGGATCAAGATAGTTTCAAGAGTGACAGGGAGGGTTATTGTTTTGAGAGATACAAA
CCGCTTCCACCATTTCAAGAAGTGCATGCTCTTGTAATGATTACTGGTGAAACCATTATACCAGAGCATAA
TTCTTTGAACCTTTTTATCTTTATTTCTCTTTGATGAGTCCATCGGCATGATCATACTACAATGCGATGCT
AGAAAAAAACAAAAAATGGCCGCCTCGGGCATCGATAAGCTTGAATCTCTAGAGTCTGCTTGAATGGAAAT
TGGCGAAGACGCTGA

**Figure B2.7:** Anchoring sites for qRT-PCR 1fox46-1 specific primers within the fl-cDNA insert of CHLOROPLAST RNA EDITING FACTOR 3 (CREF3) gene sequence.

GGAGAAAGGAGTGTTTATTTCGATTGGGAAGACTGAAGCTTTGGCTCTCTGGTGTTCGAGAGGAGTGAAGA
TGGGTGATAAAAATGATGGACTGGGCTTGAGTTTGAGCTTGGGATTCGATGGTACACAACCAAATCATCAA
CAGCAGCTTTCTATGAAGCTAAATCTCATGCCCGTACTTTCACAAAACAATCATAGAAAAACTTCCTTGAC
TGACCTCTTTCAATCATCAGATAGAGCATGTGGTACGAGGTTTTTTCAACGAGGAATTGACATGAACAGGG
TGCCAGCTGCAGTGACAGATTGTGATGACGAAACTGGGGTTTCTTCACCAAACAGCACGCTATCCAGCTTA
AGTGGTAAAAGAAGCGAAAGAGAACAGATTGGAGAAGAAACAGAAGCGGAGAGGGCCTCTTGCTCTCGTGA
CAGTGATGATGAAGATGGTGCTGGTGGTGATGCTTCTAGGAAGAAGCTGAGACTCTCAAAGGAACAGTCTT
TAGTGCTTGAAGAGACTTTCAAGGAACATAATACTCTTAATCCCAAGGAGAAGCTGGCTTTGTCAAAGCAG
TTGAATCTCAGGCCTAGGCAAGTGGAGGTGTGGTTTCAGAACCGAAGAGCAAGGACCAAGTTGAAGCAAAC
TGAAGTCGACTGCGAGTACCTAAAGAGGTGCTGTGAAAATCTAACAGAGGAGAACAGGAGGTTACAGAAGG
AGGTGCAAGAGCTTAGAGCACTGAAACTTTCCCCTCAGCTCTACATGCACATGAACCCTCCCACCACCCTC
ACCATGTGCCCTTCATGCGAGCGCGTTGCTGTCTCGTCATCTTCTGCTGCTGCCGCGTCCTCTGCTCTTGC
TCCAACTGCCTCAACCCGGCAACCACAACGACCGGTGCCCATTAACCCTTGGGCAACAATGCCCGTCCACC
ATCGAACTTTTGATGCTCCTGCTTCCAGGTCATGATTGTTAGCTTGAAGTAGGGGCTATTTGGTAAAGATA
AAATGGATGAAAGGATTTAGGATAAGATTTCCAGGCATCCACAGAAATTTGAGAGAATGTGGAATAGGGAG
AATATGAAATAAGACACGATCAGTGGTGGTAGTGGTTAGGATGTGATTTTGCTGACAAGTCCAGGTTGCAA
AGAGTGGACTAGTTGCAAAATATAGTGTTTATAAGTTGTAGGATGATTGGAAGGTGCGACAAAGGAATCCG
AATACAATATCTCCCTGCTGATTATTGTAGGATTTGATGTAGACAAAGTTGCTTTACTATGTAAAGAGAAT
AGTATTTTAGTGATCCAAAAAAAAAAAAAAAAAAAAAGGCCGCCTCGGCCATCGATAAGCTTGGATCCTC
TAGAGTCCTGCTTTAATGAGATATGCGAGACGCCTGACCCAGCTTTCTTGTACAAAGTTGGCATTATAAGA
AAGCATTGCTTATCAATTTGTTGCAACGAACAGGTCACTATCAGTCAAAATAAAATCATTATTG

**Figure B2.8:** Anchoring sites for qRT-PCR 2FOX1-1 specific primers within the fl-cDNA insert of HOMEOBOX-LEUCINE ZIPPER (HAT4) gene sequence.

ATGTAAAAAAAGGTTAATTTCATATGATGGGTTGGCTTTGAGGTTTAATTTCTTTTAGCGGTCTTGTTCTT
GTAAATCTATTTTGGGCTTTAATTGTTTAGAGTGAGAACTTGAAGACATCAGACTGGCTTTGGTTGCTGGA
AATAGATCAAATGGCTCCAAGAGATAGAGATTTTGAGGTTGATCTTGAAAGTGGGGTGAGAAATAGTGTTG
AAGATTCATGTAAAAATGCAGGTTCAGGAGTAAAAACACCAACAAAGCCGTTGCTTGCTAAGATTTGTGGG
GCATTCGCCAATGGGACAGCCAATGGTGAAGAGAGGGTAAATTTGTGTGGCAACGTGTCAGACTCTGGTGG
TGATTCTGCAGACCATGCGAAGTCGGAGGGTGAAATATCTGTTGATCAAGTAGAGAAGAAAATGGTAAAAA
AGAAGCATAAAAAAACGAGCAATAAAAAGCCTCCTAGGCCTCCACGAGGTCCATCATTGGATGCTGCTGAC
CAGAAGCTGATCAAGGAGATTTCTGAACTAGCCATGTTGAAGCGTGCAAGGATTGAGCGGATGAAGGCCTT
GAAGAAATTAAAAGCTACGAAGCCATCATCCAATAACAATCTATTTGCCATGGTGTTCACCATTCTATTCT
GCCTTGTGATTCTCTTTCAAGGAATGTCATCCAGAGCTACATCTGCAAGCTCAATGGGATCTCCTGTGTCA
TCAGAGACAGCTGGTGATGTTTATTTCAGTTCATACTTTGGGATCCATCTGCAAGCGAGTCTAATGGACTG
GGTCTGGGATATCGAACCTTCATAGAAAACCATGCTGGTTCGATCTCCTAAATTCAGGACTGTGAGATGGA
GTGGGTAAAGAAGGACCGTTACCTGTTAATCAAC

**Figure B2.9:** Anchoring sites for qRT-PCR 2fox5-2 specific primers within the fl-cDNA insert of a transmembrane gene sequence.

GAGTTGGGAGATGATATTCCGTCTTTGCCAGAGGGCAAAACACCATCCCTTCTGATGCCTCCAGCCCCTAT
TATGTGCGGTGGTGATTGGCCACTTCTGAGAGTTATGAAAGGTATATTTGAAGGTGGGCTGGATAATATGG
GCAAAGGTGGTGCTGATGAGGACGAAGAAGCTGCTGATGGTGACTGGGGTGAGGAACTGGACATGGTCGAT
GTGGATGGTTTGCAAAATGGGGATGTCTCAGCAATTTTGGAGGATGGGGAAGCAGCTGAAGAAAATGAAGA
GGAGGGAGGATGGGACCTTGAAGATCTGGAGCTACCTCCCGAGGCAGACACACCAAGGGCTTCTGTCAGTG
CCCGCTCATCAGTTTTTGTGGCTCCAACTCCTGGTATGCCTGTAAGTCAGATTTGGATTCAGAGATCTTCA
CTCGCTGCTGAACATGCCGCAGCTGGCAATTTTGATACGGCTATGCGACTACTCAACAGACAACTTGGAAT
TAAAAACTTTGTCCCGTTAAAGTCCATGTTTCTTGATCTTTACTCAGGCAGCCATACCTATCTTCGTGCAT
TTTCATCCACCCCAGTGATATCAGTGGCTGTTGGAGCGGGGATGGCAATGAGTCTGCCAGCCCTAATGTTA
GGGGTCCTCCAGGCTCTGTGTTCAATTTCTCCTCACTTGGAAAATAAGCTTACGCTGTACTAAGGCCACGA
CAACTGGGCAATTTGACTGAAGCACTAAACTCTTCCTTTGGCATTCTGCAACGATTCTCTGGATCTGTTCG
TTGATCACGATGCAGTGCATGATTCAACGAATTGATTATATAGTCAACAGTAGCTTTCGGATCTGCAATCG
AACTAAAAGAAAGCAGATGAAATG

**Figure B2.10:** Anchoring sites for qRT-PCR 3fox10-5specific primers within the fl-cDNA insert of coatomer alpha subunit gene sequence.

ATATAAAAAAATTGGCAATCCCTAGAGCAGAGCAAGATAGGCCTAGGTTTGCCTTGATCTAAACTCTATCT
CACTCACTCTCATTCACACTCTGGGCTACACAAGACAGAAGAACAGAAGCACCACCATGAGCTCAACCCGA
AGGCCCTCCCTCGCCTCCAAGCCCCGTCACTCGTTCTCTCCGCCGTAGAATGGACATCAGCACTGCCACTC
TGAAACGCTGCGGCTGATCTCTGCACCATTACTCTCCTTTCTTCTGAGGTTCAAATGGAGGTAATTGTTAA
TAAGAAGAAGCGTAGAAAGGAGCAACGAGAGAGCAATAATAATAATAATCAATTGCGTGTTTCTTCGAGCA
CTCCACGCACGCGTTCTCAGGTTTCCCCGGAGTGGACAACTAAAGAAGCGTTGATTCTAGTGAATGAGATC
GTTGCTGTTGAAAAAGATTGTTTGAAAGCCTTATCTACCTATCAGAAATGGAAGATCATTGTCGATAACTG
CGTTGTCCTGGATGTTTCCCGGAATTTGAATCAATGTCGGACCAAGTGGAACTCTTTAGTTAATGAGTACA
ACCTGATTAAAAATTGGGACAAGGAGTCTGAGTCCCGAAGTGATTTCTATTGGTCTTTGGAGAGTGAAAGG
AGAAAGGAGTTCGGACTGCCAGAGAATTTTAATGATGAACTTTTCAGAGCTATTGATGATTATATGTGGGT
GCCACAAGGAACACGCAGATACGGATGCTGGATCCAGATCCAGATCCAGATCAGATACTGACTCTGAAGTC
TTGACTTGCTTCATGCAATACAAGCCTGGGAACAGAATCAACGTGCGTCCAAGTCTCTGAATATCCCTATG
GGAAGAAAAGAACCCAGCGAATGC

**Figure B2.11:** Anchoring sites for qRT-PCR 3FOX10-7specific primers within the fl-cDNA insert of HARBINGER TRANSPOSON DERIVED PROTEIN 2 (HDP2) gene sequence.

AGGGGTTGAAGCGGAGAAAAGATGTGCTCTAGTTAAAGCGTGGGAAGAAAATGAGAAAGCTAAAGCGGAGA
ACAAGGCTCACAAGAAACTCTCTGCCATTGGATCATGGGAGACAATCAAGAGAGAGTCTGTGGAGGCAAAA
ATAAAGAAGTATGAGGAAAAAGTGGAAAAGAAGAAGGCTGAATATGCAGAGAAAATGAAGAACAAAGTAGC
CGAACTCCACAAGGCAGCCGAGGAGAAGAAAGCAATGATTGAAGCAAAAAAAGGCGAGGACCGTCTCAAGA
ATCCATTTATCGCCAGAGGAATCCAGCTAGTCTAGAGATGCAGGGAACTGGGAGAGGGCATGAACGAATGA
TAGACCTTCATGGGCTGCATGTAACTGAAGCCATTCACGTGCTAAAGCACGAGTTGAGTATTCTGAGGAGC
ACAGCACGGGCAGCAGATCAGTGTTTGCAGGTTTATATATGTGTTGGAACGGGCCATCACACTAGGGGTGC
TCGCACTCCCGCAAGACTTCCAGTTGCTGTACAGCGATACCTGCTCGAAGAAGAGGGCCTTGACTACACTG
AACCACAGCCAGGGCTGCTTCGAGTAGTGATGTATTGAACCAGCGTCACAGCAGCATGATGAGGTATAGGA
GTTTTTTGACACAATGCAAAACCCAAGCCATAGTCATCAAATCATTCTGTATCTGTATATGGGAGATATTG
AAGAAGAAGTAGTCGAAAGCTGAAAAATAAAAAAGAGAAAAATGTGAGTTAGGAAAGTAAAGACGGAGCAG
AGTGTATCATAGTGTACAGGTGACGCGATTACATTTTGTAAGCGATCAGGCACCTACATGGGAGGCCGGAC

**Figure B2.12:** Anchoring sites for qRT-PCR 3FOX12-7specific primers within the fl-cDNA insert of CTC-INTERACTING DOMAIN 7 (CID7) gene sequence.

GGACCCGAACAAGCAGAACAGGGCAGACAACCCATTCTTTCTTTCTGCAAAATCAAAAACTATAATACAGC
AGCGCCATGATCAGCATCCTAGCTCAAGAGCGTCTGCTGGGCGCCGCATTGGGAGCTGCGTTTGCGGGTTT
CATTGTTTATGAGCAACGAAAGCGCATCTATCAATCCATTTCACCCGAACATCCCCAATCCCAGTTGAGAG
AGCCCATATTTGGAAAGCAATTTCGTTCAGAGTTCGAACTTGCTTGGAACAAAGCTGTGGACCAGACATTT
GGACCTCTGGTTGCTTCTCTTAATTCACGTAGGCATTAAGACTTTGGATTAGTTTCATTGCTATTGATTTA
ACATTTATATCAAGTTCTGAGCCATGTACATGCAATAGTTCTAAATCATTTCATGGGACGTGTTCTGAGGC
TGACTATGATTGAAACTCAAATAATATATTACCTCACTTGTAATATTTTGGAATTTTAAACAACTTGTATG
GCATGGCTTATTTTCTTGTAATATTTTGGAATTTTAAACAAGCTGCATGACATGGCTTATTTTCTCCTTAA
AAAAAAAAAAAAAAAAGGCCGCCTCGGCCATCGATAAGCTTGGATCCTCTAGAGTCCTGCTTTAATGAGAT
ATGCGAGACGCCTGACCCAGCTTTCTTGTACAAGGTGTGGTCCCAAAACACACAG

**Figure B2.13:** Anchoring sites for qRT-PCR 3FOX16-5specific primers within the fl-cDNA insert of a C3HC4 type family gene sequence.

GGCTAAGCTTGTGTGGTGCTGGTGGGTCACTTATAGGGGTGGAGACGGAGAGGGTATTTCTTCAAGACACA
GTTGTTGTTCTTTGTTTTCTGGGAAAGAAGGGGAGAGGGAGAGGGAAATGGATGTGGAAATGAAGCAATCG
AGATTTAAAAGGATTTGTGTGTTTTGTGGTAGTAGTCCGGGAAAGAAAAGCAGCTATAAAGATGCTGCTAT
TGAGCTTGGAAAAGAATTGGTATCAAGAAATATTGACCTGGTTTATGGAGGAGGGAGTATTGGTTTAATGG
GGTTAATTTCTCAAGCTGTTTTTGATGGTGGCCGTCATGTGATTGGAGTTATCCCCAAGACACTCATGCCT
AGAGAGATCACTGGAGAAACAGTAGGTGAAGTGAAGGCTGTTGCTGATATGCACCAAAGGAAGGCTGAAAT
GGCTAGACATTCCGATGCTTTTATTGCCTTACCTGGTGGCTACGGGACCCTTGAAGAACTGCTTGAAGTCA
TAACTTGGGCCCAGCTTGGCATCCATGACAAGCCGGTGGGATTGCTGAATGTGGATGGATATTACAACTCC
CTGCTGTCATTCATTGACAAAGCGGTAGAGGAAGGCTTCATCAATCCAAGCGCACGCCATATAATTGTATC
CGCCCCCACCCCAAGAGAGCTTGTCAAGAAAATGGAGGAGTATTTTCCACGACATGAAATAGTGGCCTCAA
AGCTAAGCTGGGAGATTGAACAGTTAGGCTACCCTCCACAATGTGATATCTCAAGGTAAGATCGTGGCCCG
GTTATGACAAACTATGCAAATAGATTGAAGAGATTATACTGGCGGATCCAGAGTGTTGTTTAGGAAGAGAC
ATGGACCTCCAGAATATTTACCCCAAGAAGATGAAATAAAAAAACCTTGTTTTGCCAAAAAAAAAAAAAAA
AAAAAAAAAAAAAAAAAAAAAAAAAAAAGGCCGCCTCGGCCATCGATAAGCTTGGATCCTCTAGAGTCCTG
CTTTAATGAGATATGCGAGACGCCTGACCCAGCTTTCTTGTACAAAGTTGGCATTATAAGAAAGCATTGCT
TATCAATTTGTTGCAACGAACAGGTCACTATCAGTCAAAATAAAATCATTATTTGCCATCCAGCTGATATC
CCCTATAGTGAGTCGTATTACATGGTCATAGCTGTTTCCTGGCAGCTCTGGGCCGTGTCTCAAAATCTCTG
ATGTTACATTGCACAAGATAAAAATATATCATCATGAACAATAAAACTGTCTTGGCTTACATAAACAGTAA
TACAGGGGTGTTATGGAGCATATTCAACGGGAAACGTCGAGGGCGCGATTAATCAACATGAATGCTGATTA
TTGGTTAAATGGCTCGGCGAATATGTCGGCATCAGTGCCACATTCTTATCGCTTGTATGGAGCCGATGCCT
AAGTGTTTTCGGAACTGGCCAA

**Figure B2.14:** Anchoring sites for qRT-PCR 3FOX16-6specific primers within the fl-cDNA insert of LONELY GUY 1 (LOG1) gene sequence.

GATTTTCAGAGAAAGAGAGCCTTTTGGTTTGGTTTTAGCAGGTGGTGTGTTTTTTCTTTTCGGGCTTTGTT
AATGGCAGATAGAGTTGGTATACTGGTTAAAAGCATTTGCTGAAGAGAAGCAGGGAGTTTGATGTGCTGTT
GGCGTTGGCTTTTGTTCAGTGCAGATTGGGACTGCTCAGTAGCTCTTGATAAGCTTTTGCTTGTCTTGGGT
TTCTTTTGTTGGCTTAGTACCACAAGTGATTCTCGAGTTATTTATGAGCTTTACTACCTGTTATGGTGGAA
GAAAAGGTTTGCTAACAAAGAGATTGGAGATGATTACAGCAGCCCGGCGAGAGAGCTCTTCTTTATGTTCT
GTTTAAGAAAGCCATCTTCTTTAAGGAACAATCAAGAACTATGTTCATCAGTGAGAATAGCAGATGCACTT
GTCCATCACGACCAAGAATCCCAGCTCGATGTTAATACAGGCAAAGATATATTGCTCCGGTCCTGGAGCGA
TGACAATGTGGAGACAGAGCTCATGAGGCTGCATAGTCTCTCAGGTCCGCCAAGATTTCTCTTTACAATTG
TTGAAGAAACAAAGGAGGACTTGGAGTCTGAAGATGGCAGGTCTAGAGGTGATCCTAAGAGTGCGAAAGGA
TCAAGAAGTAGAAGCTTAAGTGATTTGCTTCGTACTGTGGAGACTCCATATCTAACCCCTCTTTCTTCTCC
ACCATTTTTCACACCTCCTCTTACTCCTAACTATAATCAGATTGGATTCAATCATCTCTTTGAATCGTCAA
AAGATGCAGAGTTCAATAAGATAAGATCATCACCACCTCCAAAATTCAAGTTCTTACAGGATGCGGATGAG
AAACTACATAGAAGGAAATTGATGCAAGAAGCTGGGGAGAAGGTCCAAAGGCATGATGTTTTTGCTCAGGA
TCATACCAAAATACCTGCTAGTTCTAATTCTCACAAAGACGAGGATGATGGGCCTTTTATCACC

**Figure B2.15:** Anchoring sites for qRT-PCR 3fox90-3.1 specific primers within the fl-cDNA insert of a transmembrane gene sequence.

GAAACCCAGAAGTCTAGATTCTCACGCTTTATAAAATTAACAAATAAATAAACCCCACTTTCCTAGCTCCC
ACTGTAGAATTTTCCTTCTACCTACTCTGTTCATATTCTGAAACTCCAATTCTAGTGAGGTTTCTTCTCCT
TTCAAGTTTTCTTTGCTTCCCGCAGTCCTTGTTTTCCAAAACATGTCATCTATACTAACCTCACAAGGTGT
GGTATTAGCCACAGTCATGGCAGTTTCAAGTACGGTGGTCTTTCTTGCCTTTTCCAAGCAAAAAACGTTGC
CCCATCAAGTACTCTCTGAGAATCGAGATTCCGAATCTCCGACTCCAAGTCAAGACTTGCGTTCTTGCTTA
AGTTCAGAGGGAAAGAGAAAGAAGAAGAGAGTGCAATTTGCAGAGAATGTGAAGAATACAAAAGGGAATGG
TGATGAGTACAGAAGGGAGAGGCAGAGTCCCTGGCATGCTAGGCGAGAGAGAGAGGTTTCGAATACAAGAA
TGAGCAGAGTTTGCAGAAACGAAATCCAGGGAAATCATGGAATGCCAGAAAATAGGGTTGCTTTGTACAGT
GGAATTCTCGTGGACCGTGTACACAAAATGGAATGTTCATATTTATTTCAGTAAATTCTTGGGTAATTATT
ACCTCAACTTTTCCTCTAGAAAATGTGTATATGTGAAGGGAGGCTCTGTTATTTTAATGCATCAGAGCCTT
TTCCATATTATGGATTTAAAGTCGAATTATTGTGTACAGAAGTTTATGGAGTTCCTGGATTTTTCAATTTT
AAAAAAAAAAAAAAAAGGCCGCCTCGGCCATCGATAAGCTTGGATCCTCTAGAGTCCTGCTTTAATGAGAT
ATGCGAGACGCCTGACCCAGCTTTCTTGTAACAAAGTTGGCATTATAAGAAAGCATTGCTTATCAATTTGT
TGCAACGAACAGGTCACTATCAGTCAAAATAAAATCATTATTTGCCATCCAGCTGATATCCCCTATAGTGA
GTCGTATTACATGGTCATAGCTGTTTCCTGGCAGCTCTGGCCCGTGTCTCAAAATCTCTGATGTTACATTG
CACAAGATAAAAATATATCATCATGAACAATAAAACTGTCTGCTTACATAAACAGTAATACAAGGGTGTTA
TGAGCCATATTCAACGGGAAACGTCGAGGCCGCGATTA

**Figure B2.15:** Anchoring sites for qRT-PCR 3fox90-3.2 specific primers within the fl-cDNA insert of a cytochrome P450 family gene sequence.

# C Nucleic Acid Visualization, Extraction, Amplification & Isolation

## C.1 0.7% Agarose Gel Electrophoresis

| Components | 50 ml volume |
|---|---|
| 1x buffer TAE | 50 ml |
| Agarose powder | 0.55 g |

The components combined in an Erlenmeyer flask and heated using a microwave until agarose dissolved completely. 2 drops of concentrated ethidium bromide (EtBr) was added to the 0.7% agarose TAE solution (F.8). The solution was poured into a cast and allowed to cool until solidified. The agarose gel was placed in an electrophoresis chamber and submerged in 1x TAE buffer. Nucleic acid samples mixed with appropriate amounts of visualization dyes and loaded into the wells: a DNA ladder (Thermo Scientific GeneRuler 1kb plus) was loaded into at least one well so the size of the nucleic acids can be determined. Gel images captured using UVP GelDoc-IT Imaging System and VisionWorksLS software.

## C.2 QIAGEN QIAquick Gel Extraction Purification

Used protocol supplied by the manufacture (www.qiagen.com/handbooks). Concentrations checked using NanoDrop spectrophotometer.

## C.3 Modified Genomic DNA (gDNA) Extraction

| **Extraction Buffer 1 (EB1)** | **200ml Total Volume** |
|---|---|
| NaCl 2.5 M | 40ml |
| EDTA 0.5 M | 20ml |
| TrisHCl 1M | 20ml |
| Water | 120ml |
| PVP | 4g |
| **Extraction Buffer 2 (EB2)** | **25ml Total Volume** |
| EB1 | 20ml |
| 10% SDS | 2.5ml |
| β-ME | 25µl |
| QIAGEN RNaseA | 13µl |

gDNA was extracted from leaf tissues of transformed and wt 717. Leaf tissues from in vitro grown plants were sampled and stored in a 1.5ml microcenterfuge tubes containing two glass beads. The sampled leaf tissues were immediately frozen with liquid nitrogen and stored at -80$^{o}$C until further processed. Using the TissueLyser, the frozen tissue was disrupted for 1 minute at 30 hertz and subsequently frozen with liquid nitrogen. To insure tissue disruption (repeated twice).

A volume of 450 µl of EB2 buffer was added to the disrupted leaf tissue, and the suspension was placed on a 65°C heating block for 15 minutes. A volume of 125µl 2M potassium acetate was added to the suspension, mixed thoroughly through vortexing, and placed on ice for 15 minutes. The suspension was centrifuged at maximum speed for 20 minutes.

A volume of 200 µl of chloroform:isoamil alcohol (24:1) was added to the supernatant and mixed thoroughly via vortexing. The mixture was centrifuged at 10k rpm for 5 minutes to separate the chloroform organic layer from the isoamil alcohol layer. The chloroform bound DNA was transferred to a new 1.5 ml microcentrifuge tube without disturbing the interface (repeated twice).

The gDNA was precipitated using 400µl of isopropanol. The precipitated DNA was pelleted by centrifugation at top speed for 5 minutes: the liquid was decanted and the pellet was dried. The DNA pellet was washed with a 700µl volume of 70% EtOH, mixed by vortexing, and centrifuged: the liquid was decanted and the pellet was dried. The DNA pellet was resuspended in 35 µl of DNase free water. The concentration and purity of gDNA samples checked using NanoDrop spectrophotometer. gDNA samples visualized using the electrophoresis protocol (C.1).

## C.4 Modified RNA Extraction

| **DNase Master Mix** | **10x RXN** |
|---|---|
| RDD Buffer | 700 µl |
| DNase | 100 µl |

RNA was extracted from various tissues of transformed and wt 717 hybrid poplars. Sampled tissue were placed in 1.5 ml microcenterfuge tube containing 2 glass beads, immediately frozen with liquid nitrogen and stored under -80$^{o}$C until further processed. Using the TissueLyser, the frozen tissues were disrupted for 1 minute at 30 hertz and immediately frozen with liquid nitrogen (repeated twice).

A volume of 500µl volume of RLT buffer with (PVP) (0.1g/ml) was added to the disrupted tissue and immediately vortexed. A volume of 200µl 5M potassium acetate was added to the suspension and mixed through inversion. The suspension was centrifuged at a maximum speed at 4°C for 20 minutes.

The supernatant was transferred to QIAshredder Spin column and centrifuged for 2 minutes at 4°C. The QIAshredder column was discarded and the flow through was transferred to a new 1.5 ml microcenterfuge tube containing 250 µl of 100% EtOH. The solution was mixed by inversion, transferred to an RNeasy mini spin column and centrifuged at 4°C for 1 min. A volume of 350 µl RW1buffer was applied to the RNeasy mini spin column and was used to wash the column with a 1 minute centrifugation at 10K rpm. Residual genomic DNA removed by on column digestion. A volume of 80µl DNase master mix (see above) was directly applied to the column and the reaction was allowed to proceed for 10 minutes at room temperature. The DNase reaction terminated by a second 350µl RW1 buffer washing step.

A volume of 500µl RPE buffer was then applied to the RNeasy mini spin column and centrifuged at 10k rpm. The purified RNA eluted from the column using a volume of 35µl DNase free water by 1 minute centrifugation at max speed. The concentration and purity of RNA samples checked using NanoDrop spectrophotometer. The RNA integrity checked using the electrophoresis protocol (C.1).

## C.5 QIAGEN Miniprep Plasmid Extraction

Used protocol supplied by the manufacture (www.qiagen.com/handbooks). Concentrations checked using NanoDrop spectrophotometer.

## C.6 QIAGEN Maxiprep Plasmid Extraction

Used protocol supplied by the manufacture (www.qiagen.com/handbooks). Concentrations checked using NanoDrop spectrophotometer.

## C.7 Thermo Scientific RevertAid RT cDNA Synthesis

| **RNA mix** | **12 µl total volume** |
|---|---|
| Total RNA | 0.1 ng |
| Oligo dT (2 µM) | 2 µl |
| DNase free water | Bring to volume |
| **RevertAid RT MM** | **10x RXN** |
| 5x Reaction Buffer | 40 µl |
| RiboLock inhibitor (20 U/µl) | 10 µl |
| dNTP Mix 50 µM | 20 µl |
| RevertAid RT (200 U/µl) | 10 µl |

| **Steps** | **Temperature** | **Time** | |
|---|---|---|---|
| Annealing | 42°C | 60 minutes | 2x |
| Extension | 45°C | 30 minutes | 2x |
| Denaturation | 70°C | 10 minutes | 2x |
| Hold | 4°C | ∞ | |

RNA was first denatured by incubation of the 'RNA mix' for 5 minutes at 65°C in a PCR tube and then immediately placed on ice. A volume of 8 µl of RevertAid RT master mix was added to the 12µl of denatured RNAs and using the cDNA synthesis program single stranded complementary DNAs (cDNA) were synthesized.

## C.8 Thermo Fisher DreamTaq Green PCR

| **Reaction Components** | **20 µl total volume** |
|---|---|
| 10x green DreamTaq master mix | 10µl |
| Primer 2 µM | 2 µl |
| DNA template | 500 ng |
| DNase free water | Bring to volume |

| **Steps** | **Temperature** | **Time** | |
|---|---|---|---|
| Hold | 94°C | 2 minutes | |
| Denaturation | 94°C | 15 seconds | 30x |
| Annealing | 55-60°C | 30 seconds | 30x |
| Extension | 68°C | 1.5 minutes | 30x |
| Extension | 68°C | 5 minutes | |
| Hold | 4°C | ∞ | |

PCR amplicons visualized using electrophoresis protocol (C.1).

## C.9 Thermo Fisher Platinum Taq DNA PCR

| **Reaction components** | **25 µl total volume** |
|---|---|
| 10x high fidelity PCR buffer | 2.5 µl |
| Primer 2 µM | 2.5 µl |
| $MgSO_4$ 50 µM | 1 µl |
| dNTP Mix 50 µM | 0.5 µl |
| Platinum taq (5 U/µl) | 0.25 µl |
| DNA template | 500 ng |
| DNase free water | Bring to volume |

| **Steps** | **Temperature** | **Time** | |
|---|---|---|---|
| Hold | 94°C | 2 minutes | |
| Denaturation | 94°C | 15 seconds | 30x |
| Annealing | 55-60°C | 30 seconds | 30x |
| Extension | 68°C | 1.5 minutes | 30x |
| Extension | 68°C | 5 minutes | |
| Hold | 4°C | ∞ | |

PCR amplicons visualized using electrophoresis protocol (C.1).

## C.10 QIAGEN SYBR qRT-PCR

| **Reaction components** | **20 µl total volume** |
|---|---|
| 2X SYBR Green PCR MM | 10 µl |
| Primer 2 µM | 2 µl |
| cDNA Template (5x dilution) | 100 ng |
| DNase free water | Bring to volume |

| **Steps** | **Temperature** | **Time** | |
|---|---|---|---|
| Hold | 95°C | 10 minutes | |
| Denaturation | 95°C | 15 seconds | 40x |
| Annealing/Extend | 60°C | 1 minute | 40x |

ΔΔCt analysis used to determine the relative expression levels of different genes. Instructions for how to conduct this analysis detailed with the webpage (http://sabiosciences.com/manuals/IntrotoqPCR.pdf).

# D DNA Digestion & Ligation

## D.1 Restriction Digestion

| **Reaction Components** | **50 µl total volume** |
|---|---|
| Restriction enzyme | 10 units (1µl) |
| Template DNA | 1 µg |
| 10X NEBuffer | 5 µl |
| DNase free water | Bring to volume |

| **Restriction Digestion Program** | **Temperature** | **Time** |
|---|---|---|
| Enzymatic reaction | Variable | 1 hour |
| Enzyme inactivation | 65°C | 20 Minutes |

The reaction components mixed on ice in PCR reaction tubes. The reaction conducted with a PCR machine using the reaction digestion program listed above. The reaction temperature was dependent on the specific restriction enzyme. Restriction digestions can be performed with multiple restriction enzymes. The success of the restriction digests were checked using 0.7% agarose gel electrophoresis protocol (C.1).

## D.2 NEB T4 DNA Ligase Protocol

| **Reaction components** | **20 µl total volume** |
|---|---|
| T4 DNA ligase buffer (10x) | 2 µl |
| Vector DNA | 0.020 pmol |
| Insert DNA | 0.060 pmol |
| T4 DNA ligase | 1 µl |
| DNase free water | Bring to volume |

| **T4 ligase program** | **Temperature** | **Time** |
|---|---|---|
| NEB T4 reaction | 25°C | 10 minutes |
| Inactivation | 65°C | 10 minutes |

## D.3 Gateway BP Clonase II Protocol

| **Reaction components** | **8 µl total volume** |
|---|---|
| PCR products with attB tails | 150 ng |
| pDonr221 vector (150ng/µl) | 1 µl |
| TE buffer | Bring to 6 µl volume |
| BP Clonase II enzyme mix | 2 µl (added last) |

The BP reactions incubated at 25°C for 1 hour. Proteinase K solution was added to inactivate BP clonase II and end the reaction: this step was incubated at 37°C for 10 minutes. Reaction checked using restriction digestion protocol (D.1). DNA fragment size predicted using ApE software.

## D.4 Gateway LR Clonase II Protocol

| Reaction components | 8 µl total volume |
|---|---|
| Destination Vector (150 ng/µl) | 1 µl |
| Entry vector | 150 ng |
| TE buffer | Bring to 6 µl volume |
| LR Clonase II enzyme mix | 2 µl (added last) |

The LR reactions were incubated at 25°C for 1 hour. Proteinase K solution was added to inactivate BP clonase II and end the reaction: this step was incubated at 37°C for 10 minutes. Reaction checked using restriction digestion protocol (D.1). DNA fragment size predicted using ApE software.

# E Transformation Protocols

## E.1 Heat Shock Transformation

A 50µl aliquot of *DH10B-T1$^R$ E.coli* and 0.1 µg of respective plasmid DNA were combined and incubated on ice for 30 minutes. After incubation, the cells were placed on a 42°C heating block for 30 seconds and immediately placed back on ice. A volume of 250 µl of SOC media was added to the cellular suspension and the heat shock treated DH10B-T1$^R$ cells were grown at 37°C for 1 hour in the shaker incubator. The 20 µl of heat shock treated DH10B-T1$^R$ cells were plated on specific selective media to select for transformation. The plates were incubated at 37°C overnight

## E.2 Freeze Thaw *Agrobacterium* Transformation

A 50µl aliquot of chemically-competent *Agrobacterium, AGL-1* cells, was mixed with 0.1 µg of destination binary vector and were frozen in liquid nitrogen. The frozen cells were placed on a 37°C heating block for five minutes and immediately placed on ice. A 1ml volume of LB (lenoix) liquid media (F.4) was added, incubated at 28°C for 4 hours with gentle agitation and plated on selective LB (leonix) media (F.3). Successfully transformed colonies appeared after 2-3 days incubation at 28°C.

## E.3 Glycerol Stock Preparation

After confirmation of transformation, a 500µl aliquot of either transformed *AGL-1* or *DH10B-T1$^R$* cells within LB liquid media was added to 500 µl of 50% glycerol solution in a 2 ml microcenterfuge tube. The glycerol stock was frozen with liquid nitrogen and stored in -80°C.

## E.4 Poplar Transformation

wt 717 poplars transformed using *Agrobacterium* with the method described by Han et al. (2000).

# F Growth Media & Stock Solutions

## F.1 LB (Miller) Plating Media

| Components | |
|---|---|
| Agar | 1.6 g |
| LB (miller) | 2.5 g |
| Water | 100 ml |

LB (miller) and agar were combined with water in 500 ml Pyrex glass container and mixed. The mixture was autoclaved, cooled and specific stock antibiotics stocks were added to the appropriate concentrations before pouring into Petri dishes. Used for E.coli growth.

## F.2 LB (Miller) Liquid Media

| Components | |
|---|---|
| LB (miller) | 2.5 g |
| Water | 100 ml |

LB (miller) was combined with water in 500 ml Pyrex glass container and mixed. The mixture was autoclaved, cooled and specific stock antibiotics stocks were added to the appropriate concentrations. Used for E.coli growth.

## F.3 LB (Leonix) Plating Media

| Components | |
|---|---|
| Agar | 1.6 g |
| LB (leonix) | 2 g |
| Water | 100 ml |

LB (leonix) and agar were combined with water in 500 ml Pyrex glass container and mixed. The mixture was autoclaved, cooled and specific stock antibiotics stocks were added to the appropriate concentrations before pouring into Petri dishes. Used for *Agrobacterium* growth.

## F.4 LB (Leonix) Liquid Media

| Components | |
|---|---|
| LB (leonix) | 2 g |
| Water | 100 ml |

LB (leonix) was combined with water in 500 ml pyrex glass container and mixed. The mixture was autoclaved to remove contamination. The mixture was autoclaved, cooled and specific stock antibiotics stocks were added to the appropriate concentrations. Used for *Agrobacterium* growth.

## F.5 Kanamycin 50 mg/ml stock

Components

| | |
|---|---|
| Kanamycin sulfate | 500 mg |
| Water | 10 ml |

Kanamycin sulfate was dissolved into water. A 0.2 µm filter syringe was used to filter the solution. Kanamycin stocks were stored in 1 ml aliquots in the -20°C refrigerator.

## F.6 Rifampicin 50 mg/ml stock

Components

| | |
|---|---|
| Rifampicin | 500 mg |
| 100% methanol | 10 ml |

Rifampicin was dissolved into the 100% methanol. Rifampicin stocks were stored in 1 ml aliquots in the -20°C refrigerator.

## F.7 Spectinomycin 50 mg/ml stock

Components

| | |
|---|---|
| Spectinomycin | 500 mg |
| Water | 10 ml |

Spectinomycin was dissolved into water. A 0.22 µm filter syringe was used to filter the solution. Spectinomycin stocks were stored in 1 ml aliquots in the -20°C refrigerator.

## F.8 TAE buffer (50x Concentration)

| Components | |
|---|---|
| Tris base | 242 g |
| Acetic acid (glacial) | 57 ml |
| Water | 1000 ml |

The components above are combined; the buffer should be brought to a pH of 8.

# G Statistical Analysis

## G.1 Chi Square Goodness of Fit Test

Conducted to determine the significance of the frequency of a traits alteration within the mutant FOX subset. Conducted as described in chapter 10 of Carlson (1973).

## G.2 “Student’s” t-test

Conducted to determine if a measured trait showed significant difference from the wt 717 poplar. Conducted as described in chapter 10 of Carlson (1973).

## G.3 Confidence Interval

Conducted to show variability of mutant FOX line traits from the wt 717 trait mean values. Conducted as described in chapter 10 of Carlson (1973).

## G.4 Z-score Statistic

Conducted to normalize data for NetWalker 1.0 software and generate heatmap. Conducted as described by the "Data Import and Processing" tutorial page of NetWalker website (https://netwalkersuite.org/).

# H Additional Sequencing Data of Nonphenotypic FOX Lines

**Table H.1:** Functional annotation of the fl-cDNAs identified in the non-phenotypic lines. Lines with more than 1 insertion are indicated with the same line number but with the '.1' and '.2' extensions. E-values based on BLAST analysis of gene against *P.trichocarpa* genome (continued on next page).

| FOX line | E-Value | Pt Gene ID | At Ortholog AGI | Gene Name/Description |
|---|---|---|---|---|
| ***1f2-5.1*** | 0 | Potri.012G077300 | AT1G60010 | D-ribose-binding periplasmic protein |
| ***1f2-5.2*** | 0 | Potri.008G153800 | AT3G22520 | Spindle assembly abnormal protein |
| ***1f3-1*** | 0 | Potri.001G448900 | AT1G32810 | RING/FYVE/PHD zinc finger |
| ***1f3-5*** | 0 | Potri.017G087200 | AT5G39570 | PLD REGULATED PROTEIN 1 (PLDRP1) |
| ***1f3-10*** | 0 | Potri.005G055300 | AT2G30590 | WRKY DNA BINDING PROTEIN 21 (WRKY21) |
| ***1f6-1*** | 0 | Potri.017G137200 | AT3G14330 | CHLOROPLAST RNA EDITING FACTOR 3 (CREF3) |
| ***1f43-2.3*** | 2.1E-174 | Potri.017G007400 | AT2G43970 | LA RELATED PROTEIN 6B (LARP6B) |
| ***1f45-4*** | 1.7E-121 | Potri.015G122500 | AT2G35120 | Single hybrid motif superfamily protein |
| ***1f46-1*** | 0 | Porti.017G137200 | AT3G14330 | CHLOROPLAST RNA EDITING FACTOR 3 (CREF3) |
| ***1f47-1*** | 0 | Potri.008G094300 | AT3G29360 | UPD GLUCOSE DEHYDROGENASE 2 (UGD2) |
| ***1f47-2.1*** | 0 | Potri.002G015100 | AT3G03190 | GLUTATHIONE-S-TRANSFERASE 11 (GSTF11) |
| ***1f47-5*** | 0 | Potri.014G052500 | AT1G02170 | LSD ONE LIKE 3 (LOL3) |
| ***2Fox4-4*** | 0 | Potri.014G017900 | AT2G26680 | FbkM family methyltransferase |

| FOX line | E-Value | Pt Gene ID | At Ortholog AGI | Gene Name/Description |
|---|---|---|---|---|
| ***2f5-2*** | 0 | Potri.008G102700 | AT3G17120 | Transmembrane protein |
| ***2f7-1*** | 0 | Potri.018G018600 | AT4G31820 | ENHANCER OF PINOID (ENP) |
| ***2f10-2*** | 0 | Potri.004G224000 | AT1G20920 | REGULATOR OF CBF GENE EXPRESSION 1 (RCF1) |
| ***2f57-2*** | 0 | Potri.002G100900 | AT4G09020 | ISOAMYLASE 3 (ISA3) |
| ***3f10-1*** | 0 | Potri.002G158500 | AT1G01730 | hypothetical protein |
| ***3f10-4*** | 0 | Potri.008G190000 | AT1G23760 | POLYGLACTURONASE 3(PG3) |
| ***3f10-5*** | 0 | Potri.015G069700 | AT1G62020 | Coatomer alpha subunit |
| ***3f12-2.1*** | 8.2E-86 | Potri.005G199700 | AT3G03773 | HSP90 |
| ***3f12-8.1*** | 2.5E-132 | Potri.006G104600 | AT5G01650 | MIF superfamily protein |
| ***3f13-2.2*** | 3.5E-174 | Potri.002G188600 | AT3G62220 | Protein kinase superfamily protein |
| ***3f13-7*** | 2.6E-98 | Potri.009G054400 | AT5G19350 | RNA-binding protein |
| ***3f17-8*** | 0 | Potri.005G186900 | AT1G43850 | SEUSS (SEU) |
| ***3f18-1*** | 2.9E-81 | Potri.019G002500 | AT5G36930 | Disease Resistance protein (TIR-NBS-LRR class) family |
| ***3f18-6*** | 0 | Potri.010G116500 | AT1G15140 | FERREDOXIN-NADP(+) OXIDOREDUCTASE-LIKE (FNRL) |
| ***3f30-6*** | 1.2E-104 | Potri.004G053000 | AT2G33990 | IQ DOMAIN 9 (IQD9) |
| ***3f54-1*** | 0 | Potri.004G068400 | AT2G25720 | Hypothetical protein |
| ***3f90-3.1*** | 0 | Potri.008G054400 | AT5G59350 | Transmembrane protein |
| ***3f90-3.2*** | 0 | Potri.001G192800 | AT1G52565 | Cytochrome P450 family protein |
| ***3f90-5*** | 1.5E-116 | Potri.006G085400 | AT4G31180 | IMPAIRED IN BABA-INDUCED DISEASE IMMUNITY 1 (IBI1) |